of new assignments for the location of the Q_0^x transition. The assignments for some of the chlorins are somewhat equivocal because of the presence of vibrational bands with appreciable MCD intensity.

Michl's prediction[17b] of the inverted, +−+−, sign pattern for the visible and Soret MCD bands of bacteriochlorins is confirmed. In the chlorin series, we find that the specific sign pattern observed is remarkably sensitive to the particular substituents on the periphery and at the center of macrocycle. In free-base chlorin, for example, the visible but not the Soret MCD bands are inverted, whereas in octaethylchlorin the visible and Soret MCD bands show the normal, −+−+, sign pattern. In zinc octaethylchlorin the sign pattern is normal while in octaethylchlorin dication the inverted pattern is again seen. In the isobacteriochlorin system Michl[17b] concluded that ΔHOMO ≈ ΔLUMO and did not explicitly predict the sign pattern. Our MCD spectra show that the MCD sign pattern for the Q_0^x and Q_0^y transitions in the alkyl-substituted isobacteriochlorin derivatives is normal, whereas in the tetraphenylisobacteriochlorin derivatives the sign pattern is inverted. In the Soret region the sign pattern does not always follow that in the visible.

In conclusion, we believe that our results are highly pertinent to spectroscopists, chemists, and biochemists involved in the study of reduced porphyrins since they provide an adequate experimental demonstration that the MCD sign patterns of these systems depend, in general, on the substituents present. In Part 2[1b] we elaborate Michl's perimeter model[17] and show how our results can be rationalized and how further predictions can be made.

Acknowledgment. We wish to thank Professors A. Eschenmoser and A. Pelter for providing samples of 2,2,7,7,12,13,17,18-octamethylisobacteriochlorin and bonellin, respectively. We also thank Professor R. H. Holm for his interest in this project and Ruth Records for her assistance with measurements. Y.-C.L. was a visiting scholar from the Beijing Institute of Chemical Reagents. A.M.S. was a predoctoral fellow of the Fannie and John Hertz Foundation. Financial support of this research was provided by grants from the National Science Foundation (CHE-77-04397 and CHE-80-09240) and the National Institutes of Health (GM-20276 and HL-16833).

Registry No. 1a, 101-60-0; **2a**, 2683-84-3; **5a**, 82113-29-9; **5b**, 75214-81-2; **5c**, 82135-12-4; **5d**, 82166-55-0; **6**, 78023-42-4; **8a**, 71250-54-9; **8b**, 82113-30-2; *trans*-octaethylchlorin, 22862-60-8; tetraphenylchlorin, 13554-17-1; zinc chlorin, 77124-66-4; zinc octaethylchlorin, 28375-45-3; zinc tetraphenylchlorin, 14839-32-8; zinc chlorin pyridinate, 82135-09-9; zinc octaethylchlorin pyridinate, 82135-10-2; zinc tetraphenylchlorin pyridinate, 82135-11-3; chlorin dication, 82113-31-3; octaethylchlorin dication, 82113-32-4; tetraphenylchlorin dication, 50849-36-0; chlorin dianion, 55309-59-6; octaethylchlorin dianion, 38705-82-7; tetraphenylchlorin dianion, 82113-33-5; octaethylbacteriochlorin, 23016-64-0; tetraphenylbacteriochlorin, 5143-18-0; octaethylbacteriochlorin dication, 82113-34-6; tetraphenylbacteriochlorin dication, 82113-35-7; zinc tetraphenylbacteriochlorin, 50795-70-5; octaethylisobacteriochlorin, 72260-12-9; tetraphenylisobacteriochlorin, 25440-13-5; zinc octaethylisobacteriochlorin, 39001-89-3; zinc tetraphenylisobacteriochlorin, 14705-64-7; octaethylisobacteriochlorin dication, 82113-36-8; tetraphenylisobacteriochlorin dication, 82113-37-9; zinc porphine, 14052-02-9.

Magnetic Circular Dichroism Studies. 61. Substituent-Induced Sign Variation in the Magnetic Circular Dichroism Spectra of Reduced Porphyrins. 2. Perturbed Molecular Orbital Analysis[1]

Joseph D. Keegan, Alan M. Stolzenberg, Yu-Cheng Lu, Robert E. Linder,[2] Günter Barth, Albert Moscowitz,*[3b] Edward Bunnenberg, and Carl Djerassi*[3a]

Contribution from the Departments of Chemistry, Stanford University, Stanford, California 94305, and The University of Minnesota, Minneapolis, Minnesota 55455.
Received October 21, 1981

Abstract: The MCD data in Part 1 for a series of unsubstituted, alkyl-substituted, and tetraphenyl-substituted chlorins, bacteriochlorins, and isobacteriochlorins are subjected to a perturbed molecular orbital analysis in order to test the utility and applicability of Michl's perimeter model for relating the absolute signs of the four lowest-energy purely electronic MCD bands of cyclic π-electron systems to their molecular structures. A protocol is developed for this purpose which does not require explicit numerical calculations, but instead combines the elements of an experimental basis and the classic concepts of Gouterman's four-orbital model of porphyrin states in order to estimate the relative absolute size of the orbital energy differences between the two highest occupied (ΔHOMO) and the two lowest unoccupied (ΔLUMO) molecular orbitals. In the isobacteriochlorin series the splitting in the LUMO's evident from MO calculations is included in the protocol in an ad hoc manner. The MCD band sign patterns of all porphyrins and reduced porphyrins investigated are correctly predicted with the use of our protocol in conjunction with Michl's model. Particular emphasis is placed on the subtle peripheral and central substituent-induced sign variations which occur in the chlorin series. The application of the model as a useful first-order structural-elucidation technique for other systems is illustrated by reference to some naturally occurring reduced porphyrins.

The occurrence of sign and intensity variations in the magnetic circular dichroism (MCD) spectra of a series of related organic molecules suggests the possibility of developing a theoretical framework from which relatively simple rules can be elicited for relating molecular structures to their observed spectra. In our own early work we found a variety of signs, shapes, and intensities for the MCD associated with the $n \rightarrow \pi^*$ transition of saturated ketones.[4a] In later work we developed a protocol for extracting

(1) For Part 60, see the preceding paper in this issue.
(2) Surface Science Laboratory, 4151 Middlefield Road, Palo Alto, California 94303.
(3) (a) Stanford University. (b) University of Minnesota.

0002-7863/82/1504-4317$01.25/0

structural information for ketones which essentially involved projecting the perturbing atoms onto quadrant diagrams thereby decomposing the total structural perturbation into its various components, each of which transforms as a different representation of the C_{2v} point group.[4b-f]

The first observation of sign variation in the MCD bands of a cyclic π-electron system was made by Foss and McCarville,[5] who noted that the sign of the first MCD band of benzene derivatives was positive or negative, depending on whether the substituent was meta or ortho-para directing, respectively. Subsequently, Michl[6] demonstrated that this was a consequence of a theorem[6a] which stated that "within the framework of the Pariser–Parr–Pople model, the MCD spectra of two π-electron species paired in the sense of alternant symmetry are mirror images of each other". This theorem carries with it the implicit recognition of "soft" MCD chromophores as those whose MCD sign pattern is governed by the nature and location of its substituents or heteroatoms and "hard" MCD chromophores as those whose sign pattern is characteristic for the parent system and thus is not easily susceptible to change by substituents. Within this series of preliminary papers Michl[6] also formulated a rule that the signs and magnitudes of the lowest-energy $\pi \rightarrow \pi^*$ *B*-term MCD bands of cyclic π-electron systems which can be derived from a $(4N + 2)$-electron [*n*]annulene can be related to the difference between the absolute value of the energy separation of the two highest occupied molecular orbitals (ΔHOMO) and that of the two lowest unoccupied molecular orbitals (ΔLUMO).

In a more recent series of papers, Michl and his collaborators have continued their efforts to develop[7a-c] and to test[7d] simple rules for predicting the absolute signs of the MCD bands associated with the lowest-energy purely electronic $\pi \rightarrow \pi^*$ transitions of cyclic π-electron systems. A point of particular interest to us has been Michl's explicit predictions of the MCD sign patterns for the *A* term MCD bands associated with the visible and Soret transitions of symmetric porphyrins[7a] as well as those for the *B*-term MCD bands of the less symmetric reduced porphyrins[7b]—the chlorins, bacteriochlorins, and isobacteriochlorins. At the same time these predictions were made, MCD spectra had not been reported for any bacterio- or isobacteriochlorin. Furthermore, the predictions were made for the parent chlomophores themselves and possible additional perturbations due to external substituents were not considered.

Since, as noted in Part 1,[1] reduced porphyrins are of central importance to a variety of life processes and since MCD has already been widely applied to the study of many natural and synthetic porphyrins,[8] the development of rules for MCD spectra–structure correlations which can be used at an intuitive level is likely to be of general interest. In the present paper we test Michl's perimeter model against the data accumulated and presented in Part 1[1] and elaborate a perturbation treatment useful for handling the effects of peripheral and central substituents.

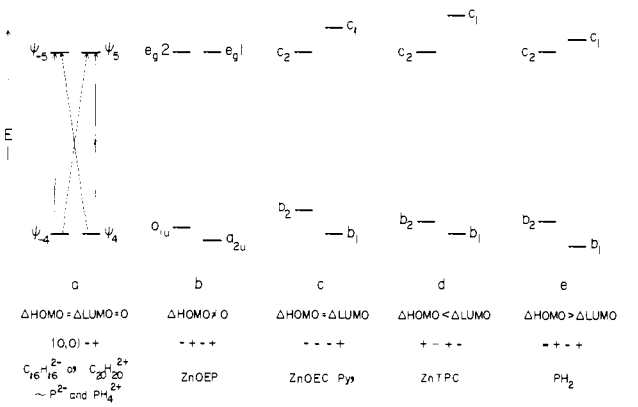

Figure 1. Illustrations, with examples, of the MCD band sign patterns (in order of increasing energy) predicted by Michl's perimeter model[7] for the separations between the LUMO (e_g1, e_g2 or c_2, c_1) and HOMO (a_{1u}, a_{2u} or b_2, b_1) four-orbital energy levels obtaining for porphyrins and reduced porphyrins.

Results and Discussion

Results and Limitations of the Perimeter Model. In this section we consider the basis of Michl's perimeter model briefly and extract those results of the model which will be useful for the nonspecialist to consider in relating the MCD spectra of porphyrins and reduced porphyrins to their molecular structures. A similar, but more broadly based, description has recently been presented by Michl[7e] and a full presentation of the model as its applies to a variety of high- and low-symmetry π-electron systems can be found in the primary references.[7a-d]

In Part 1,[1] we noted that the MCD associated with any particular transition is comprised, in the general case, of *A*-, *B*-, and *C*-term contributions, that the *C* term vanishes if the ground state is nondegenerate and thus would not be of interest for the molecules being considered, that the *A* term may be nonzero if the molecule possesses a threefold or higher symmetry axis as is the case for symmetrically substituted metalloporphyrins, and that *B* terms would be ubiquitous for the transitions of the less-symmetric reduced porphyrins. In order to develop a model which would be adequate to the problem of generating simple rules for relating the molecular structures of a wide variety of cyclic π-electron systems to their purely electronic *A*- and *B*-term MCD spectra, Michl[7] returned to the π-perimeter, or cyclic polyene, model which had been developed earlier by Platt[9] and Moffitt[10] for correlating the electronic spectra of cata-condensed hydrocarbons and which was later incorporated in the four-orbital model for porphyrins by Gouterman.[11]

Single-electron excitations between the pair of highest occupied molecular orbitals (HOMO's) and the pair of lowest unoccupied molecular orbitals (LUMO's) of an appropriate parent $(4N + 2)$-electron [*n*]annulene are considered initially. For example, $C_{16}H_{16}^{2-}$ and $C_{20}H_{20}^{2+}$ are both appropriate parent annulenes for porphyrins. The HOMO's and LUMO's are degenerate by symmetry (Figure 1a) and single-electron excitation gives rise to four singlet configurations $\psi_4{}^5$, $\psi_{-4}{}^{-5}$, $\psi_{-4}{}^5$, and $\psi_4{}^{-5}$. In the first pair of configurations the angular momentum has changed by ± 1 unit, whereas in the second pair the change is ± 9 units. Michl refers to these as sense-preserving and sense-reversing excitations, respectively, according to the physical picture in which the circulation directions of the hole and the electron are in the same or in opposite directions. The sense-preserving excitations carry with them large electric dipole moments but small magnetic moments and together give rise to the Soret, or B, transition of porphyrins. The sense-reversing excitations, on the other hand, have small electric dipole moments (zero if the HOMO degeneracy

(4) (a) Barth, G.; Bunnenberg, E.; Djerassi, C.; Elder, D.; Records, R. *Symp. Faraday Soc.* **1969**, *No. 3*, 49–60. (b) Seamans, L.; Moscowitz, A.; Barth, G.; Bunnenberg, E.; Djerassi, C. *J. Am. Chem. Soc.* **1972**, *94*, 6464–6475. (c) Morrill, K.; Linder, R. E.; Bruckman, E. M.; Barth, G.; Bunnenberg, E.; Djerassi, C.; Seamans, L.; Moscowitz, A. *Tetrahedron* **1977**, *33*, 907–911. (d) Dixon, J. S.; Linder, R. E.; Barth, G.; Bunnenberg, E.; Djerassi, C.; Seamans, L.; Moscowitz, A. *Spectrosc. Lett.* **1976**, *9*, 777–788. (e) Seamans, L.; Moscowitz, A.; Linder, R. E.; Morrill, K.; Dixon, J. S.; Barth, G.; Bunnenberg, E.; Djerassi, C. *J. Am. Chem. Soc.* **1977**, *99*, 724–727. (f) Linder, R. E.; Morrill, K.; Dixon, J. S.; Barth, G.; Bunnenberg, E.; Djerassi, C.; Seamans, L.; Moscowitz, A. *J. Am. Chem. Soc.* **1977**, *99*, 727–739.

(5) Foss, J. G.; McCarville, M. E. *J. Am. Chem. Soc.* **1967**, *89*, 30–32.

(6) (a) Michl, J. *J. Chem. Phys.* **1974**, *61*, 4270–4273. (b) Michl, J. *Chem. Phys. Lett.* **1976**, *43*, 457–460. (c) Michl, J. *Ibid.* **1976**, *39*, 386–390. (d) Michl, J. *Int. J. Quantum Chem. Symp.* **1976**, *10*, 107–117. (e) Michl, J. *Spectrosc. Lett.* **1977**, *10*, 509–517.

(7) (a) Michl, J. *J. Am. Chem. Soc.* **1978**, *100*, 6801–6811. (b) Michl, J. *Ibid.* **1978**, *100*, 6812–6818. (c) Michl, J. *Ibid.* **1978**, *100*, 6819–6824. (d) Fifteen additional papers appear in this issue of the Journal. (e) Michl, J. *Pure Appl. Chem.* **1980**, *52*, 1549–1563.

(8) (a) Sutherland, J. C. In "The Porphyrins"; Dolphin, D., Ed.; Academic Press: New York, 1978; Vol. III, pp 225–248. (b) Holmquist, B. *Ibid.*, pp 249–270. (c) Sutherland, J. C.; Holmquist, B. *Annu. Rev. Biophys. Bioeng.* **1980**, *9*, 293–326.

(9) Platt, J. R. *J. Chem. Phys.* **1949**, *17*, 484–495.

(10) Moffitt, W. *J. Chem. Phys.* **1954**, *22*, 320–333.

(11) (a) Gouterman, M. *J. Mol. Spectrosc.* **1961**, *6*, 138–163. (b) Gouterman, M.; Wagnière, G. H.; Snyder, L. C. *Ibid.* **1963**, *11*, 108–127. (c) Weiss, C.; Kobayashi, H.; Gouterman, M. *Ibid.* **1965**, *16*, 415–450.

is exact) and larger magnetic moments and together make up the visible, or Q, transition. Michl calculates the magnetic moments μ^- and μ^+ associated with sense-preserving and sense-reversing excitations, respectively, for a number of annulene perimeters and tabulates them for various net charges of the π system. The μ^- moment is small and usually negative (for $C_{20}H_{20}^{2+}$, $\mu^- = -0.53$ β_e), whereas μ^+ is always negative and much larger in magnitude (for $C_{20}H_{20}^{2+}$, $\mu^+ = -7.19$ β_e). Next, Michl considers the effects of structural perturbations which convert the parent annulene to either a molecule with a threefold or higher symmetry axis[7a] (e.g., D_{4h} for symmetric metalloporphyrins) or else to one whose symmetry is lower[7b] (e.g., C_{2v} for chlorins) and incorporates μ^+ and μ^- into algebraic expressions for the A and B terms. These expressions contain, in addition, energy differences between transitions as well as parameters which relate to the strength of the perturbation, the relative splitting of the HOMO's and LUMO's, and the symmetry properties of the perturbation. While these expressions could be evaluated numerically for any particular π-electron system of interest, the operative utility of Michl's model stems from his proposition that in most cases it is possible to predict absolute MCD band sign patterns on the basis of the relative size of the positive quantities ΔHOMO and ΔLUMO and that this knowledge can be derived from the application of qualitative molecular orbital concepts such as those of PMO theory.[12] In Figure 1 we illustrate the energy-level distributions of the HOMO's and LUMO's that are relevant to molecular systems which are derived from the porphin chromophore, and in the remainder of this section we summarize Michl's conclusions as to the MCD sign patterns that may be expected for each case.

Figure 1a illustrates the case ΔHOMO = ΔLUMO = 0 that exists by symmetry for two pertinent parent annulenes for the porphyrin ring system, $C_{16}H_{16}^{2-}$, and $C_{20}H_{20}^{2+}$. Although the μ^+ magnetic moment of the lower, L, state is high, the purely electronic A term for this state vanishes since its dipole strength is zero. B terms for the upper, B, and lower, L, states are also zero. The A term of the B state does not vanish but depends only on the sign of μ^- which is small and negative. Thus, a positive A term, i.e., one for which the sign pattern of the MCD bands is $-+$ with increasing energy, is the only nonzero MCD that is predicted by Michl's model for these annulenes. This case is very closely approximated in the spectra of porphine dianion[13] (P^{2-}) and porphine dication[14] (PH_4^{2+}). The latter derivative has a positive Soret (B state) A term and both have very weak Q_0 (L state) absorption bands along with nonzero negative A terms (i.e., the MCD sign pattern in the Q_0 band is $+-$). The occurrence of such "inverted" A terms in the MCD spectra of symmetric porphyrins is not directly accounted for in the perimeter model and Michl[7a] points out that in a more rigorous treatment vibronic effects would have to be incorporated as well. Chromophores for which ΔHOMO = ΔLUMO = 0 are thus very susceptible to the effects of weak perturbations and are termed "double soft". We will turn to a consideration of the MCD associated with other approximately double-soft porphyrin chromophores in a later paper.[15]

The energy-level situation that exists for most symmetric porphyrins is depicted schematically in Figure 1b. The LUMO's are degenerate by symmetry, whereas the HOMO's are split owing to the effects of symmetric perturbations (vide infra). In this case μ^- and μ^+ appear as linear combinations in the expressions for the A terms associated with both the Soret and Q transitions. Since μ^+ is the much larger of the two moments, the purely electronic A terms of both the Soret and Q transitions are predicted to be positive, i.e., the "normal" $-+-+$ MCD band sign pattern with increasing energy should be observed. This is, indeed, found in the MCD spectra of all symmetric porphyrins which have appreciable absorption intensity in the Q_0 band.[15] Michl also predicts that the B terms due to the mixing of the Q and B states by the magnetic field will be nonzero and that the positive Soret A term will be overlayed by a positive B term, whereas that of the Q_0 transition will have a negative B term associated with it. Since positive and negative B terms are observed in the MCD spectrum as negative and positive MCD bands, respectively, Michl predicts that the positive lobe of the MCD effect in the Q_0 transition of symmetric porphyrins should be more intense than that of the negative, lower-energy lobe, whereas the converse should obtain for the Soret transition. We confirm this prediction, experimentally, for zinc tetraphenylporphyrin but not for zinc octaethylporphyrin (where the respective lobes have the same $|[\theta]_M|$). A general congruence between experiment and theory on the B terms of symmetric porphyrins may exceed the limitations inherent in the model. Michl refers to π systems for which ΔHOMO $\neq 0$, ΔLUMO = 0 as "positive-hard" chromophores and notes that, while their MCD band sign pattern should be generally predictable, they are susceptible to becoming "double-soft" as ΔHOMO approaches zero.

In porphyrins whose symmetry is lower than D_{4h}, structural perturbations have lifted the degeneracy of their LUMO's and such systems exhibit only B terms in their MCD spectra. The "soft" case for which ΔHOMO = ΔLUMO $\neq 0$ (Figure 1c) is of particular interest since we will subsequently propose that zinc chlorins drift through this condition of equality in their relative orbital-energy differences depending on the peripheral and axial substituents present. Michl's[7b] analytical expressions for the B-term MCD associated with the low-energy transitions of soft MCD chromophores indicate that μ^+ contributions are absent. Consequently, since the B terms derive only from the much smaller μ^- contributions, the MCD of purely electronic origin for such systems is likely to be quite weak in general. This would be especially the case for the two lowest transitions on the basis of an unfavorable energy denominator since their MCD intensity arises from interstate mixing ($Q_0^{x,y}$–$B_0^{x,y}$) and not from intrastate mixing (Q_0^x–Q_0^y). Michl predicts that the electronic MCD band sign pattern for soft chromophores will be $---+$ with increasing energy. Again, the possible incursion of vibronic effects must be kept in mind, especially for electronic transitions which have little absorption intensity.

As the exact equality between ΔHOMO and ΔLUMO degrades a gradual transition is effected to one of the two "hard" MCD chromophore cases depicted in Figures 1d and 1e. The expressions[7b] for the B-term MCD associated with the four lowest-energy transitions of hard MCD chromophores are again linear combinations of the μ^- and μ^+ magnetic moments. Their relative importance depends, however, on $|\Delta\text{HOMO} - \Delta\text{LUMO}|$. If this quantity is relatively large, the μ^+ contributions will dominate and the MCD band sign pattern observed will be governed by the sign of ΔHOMO – ΔLUMO. If ΔHOMO > ΔLUMO (Figure 1e), then the normal, $-+-+$, MCD band sign pattern is predicted. This is the sign pattern found, for example, in the MCD spectra of symmetrically substituted free-base porphyrins such as that of porphine shown in Figure 2 of Part 1.[1] On the other hand, if ΔHOMO < ΔLUMO (Figure 1d), then the inverted, $+-+-$, MCD band sign pattern is predicted. The MCD spectrum of zinc tetraphenylchlorin, shown in Figure 5 of Part 1,[1] constitutes an appropriate example of the inverted case. When $|\Delta\text{HOMO} - \Delta\text{LUMO}|$ becomes small, the soft chromophore case (Figure 1c) is approached and μ^- contributions may become significant. Michl concludes[7b] that their contribution to the observed MCD band sign pattern is invariant, namely $---+$, regardless of the actual sign of ΔHOMO – ΔLUMO. Consequently, orbital-energy situations can be envisioned for which MCD effects arising from μ^+ contributions are canceled or else reinforced by those due to μ^- contributions. As noted previously, the potential for this, the "almost soft", case may exist in the zinc chlorins. In these cases, we will subsequently see that the observed MCD band sign patterns are often best explained on the basis of μ^+ contributions

(12) Dewar, M. J. S.; Dougherty, R. C. "The PMO Theory of Organic Chemistry"; Plenum Press: New York, 1975.

(13) Barth, G.; Linder, R. E.; Bunnenberg, E.; Djerassi, C. *J. Chem. Soc., Perkin Trans. 2* **1974**, 696–699. Since porphine dianion is subject to photodecomposition upon irradiation in the near-UV region, the Soret MCD could not be measured.

(14) Barth, G.; Linder, R. E.; Bunnenberg, E.; Djerassi, C. *Ann. New York Acad. Sci.* **1973**, *206*, 223–246. The opposite sign convention for the A term was used in this paper.

(15) Keegan, J. D.; Bunnenberg, E.; Djerassi, C., manuscript in preparation.

Table I. Summary of Sign Patterns Observed Experimentally and Predicted for the Lowest-Energy Electronic MCD Bands of Some Porphyrins and Reduced Porphyrins[a]

compound	free base	dianion	dication	Zn	Zn-Pyr
porphine	− + − +	+ − (x x)[b]	+ − − +	− + − +	− + − +[c]
	[− + − +]	[0 0 − +][d]	[0 0 − +][d]	[− + − +]	[− + − +]
octaethylporphyrin	− + − +[e]	− + (x x)[b]	− + − +[e]	− + − +[c,f]	− + − +[c]
	[− + − +]	[− + − +]	[− + − +]	[− + − +]	[− + − +]
tetraphenylporphyrin	− + − +[e]	− + − +[c]	− + − +[c]	− + − +[c]	− + − +[c]
	[− + − +]	[− + − +]	[− + − +]	[− + − +]	[− + − +]
chlorin	+ − − +	+ − (+)[g] − +	+ − + −	+ − (+)[g] − +	+ − + −
	[+ − + −]	[+ − + −]	[+ − + −]	[+ − + −]	[+ − + −]
	(− +)	(− +)		(− +)	
octaethylchlorin	− + − +	+ − − +	+ − + −	− + − +	(±) − − +
	[− + − +]	[+ − + −]	[+ − + −]	[− + − +]	[+ − + −]
				(− +)	(− − − +)
bonnelin dimethyl ester	− + − +	*h*	+ − + −	− + − +	+ − − +
	[− + − +][i]	[+ − + −][i]	[+ − + −][i]	[− + − +][i]	[+ − + −][i]
tetraphenylchlorin	+ − − +	+ − + −	+ − + −	+ − + −	*h*
	[+ − + −]	[+ − + −]	[+ − + −]	[+ − + −]	[+ − + −]
octaethylbacteriochlorin	+ − + (+)[j] −	*h*	+ − + −	*h*	*h*
	[+ − + −]	[+ − + −]	[+ − + −]	[+ − + −]	[+ − + −]
tetraphenylbacteriochlorin	+ − + (+)[j] −	*h*	+ − + −	+ − + (+)[j] −	*h*
	[+ − + −]	[+ − + −]	[+ − + −]	[+ − + −]	[+ − + −]
octaethylisobacteriochlorin	− + − +[k]				
	− + − −	*h*	− + − +	− + (+)[g] − +	*h*
	[− + − +]	[− + − +]	[− + − +]	[− + − +]	[− + − +]
	{− + − +}	{− + − +}	{− + − +}	{− + − +}	{− + − +}
tetraphenylisobacteriochlorin	+ − − +	*h*	+ − + −	+ − − +	+ − + −
	[− + − +]	[0 0 − +][d]	[0 0 − +][d]	[− + − +]	[− + − +]
	{+ − + −}	{+ − + −}	{+ − + −}	{+ − + −}	{+ − + −}
	(− +)			(− +)	

[a] Sign patterns are given left-to-right in order of increasing energy. Data are taken from Part 1 (ref 1) unless otherwise noted. Predicted sign patterns are given in brackets, assuming that μ^+ contributions dominate. Sign patterns in parentheses are those for the μ^- contribution. Sign-pattern predictions given in braces in the isobacteriochlorin series are based on separate considerations discussed in the text in connection with Figure 9. [b] Photodecomposition reported on irradiation in the near UV.[13] [c] J. Keegan, unreported data. [d] Prediction assumes $\Delta HOMO = \Delta LUMO = 0$, vibronic effects are not included in Michl's model. [e] Reference 14. [f] Reference 24. [g] Weak MCD band on the long-wavelength side of the main Soret band system. [h] Not measured. [i] Prediction is that for octaethylchlorin since the loss of two methyl groups is difficult to scale properly in the energy-level diagrams; see, however, the discussion in the text. [j] Intermediate shoulder. [k] Sign pattern taken from the 77 K MCD spectrum given in Figure 9 in Part 1.

for the Q bands and μ^- contributions for the Soret bands.

The limitations inherent to Michl's model stem from the fact that it operates within a four-orbital π-electron framework. One consequence of this is that explicit consideration of the MCD that may arise from the magnetic intermixing of $\pi\pi^*$ with $\sigma\pi^*$ and $n\pi^*$ states is automatically excluded. In porphyrins and reduced porphyrins $\sigma \rightarrow \pi^*$ transitions should occur at higher energies[16,17] with low oscillator strengths and their neglect seems therefore to be legitimate. An $n \rightarrow \pi^*$ transition is calculated[17] to lie within the Soret envelope but has not been unequivocally located in experimental polarization studies.[18,19] The neglect of $n\pi^*$, $\pi\pi^*$ mixing does not constitute a problem for the application of the model to azines[20] and azanaphthalenes,[21] and this neglect should not be of greater importance for porphyrins and reduced porphyrins.

A more serious problem, however, is posed by the limited number of $\pi\pi^*$ states which are considered in the perimeter model and by the extent to which the "four-orbital" states survive and dominate the Soret and visible transitions of porphyrin derivatives. Thus, the failure to include higher-energy states, even when separated from the Soret, means that the MCD associated with the fourth state may not be well predicted by the perimeter model since the contributions to it owing to magnetic mixing with the higher states are neglected. With regard to the related problem, we noted in Part 1[1] examples wherein the MCD and absorption spectra in the Soret region were more complex than allowed by the four-orbital model. Consequently, some discrepancies between experiment and theory can be anticipated for the Soret region. On the other hand, the four-orbital model does describe the composition of the visible transitions of the reduced porphyrins adequately,[16,17,22,23] and it is for them that Michl's model receives its most rigorous and general test.

Protocol for Application of the Perimeter Model. The protocol we will elaborate for interpreting the effects of substituents on the MCD of porphyrins and reduced porphyrins (as summarized, from Part 1,[1] in Table I of this paper) differs somewhat in detail from that used by Michl.[7a,b] Michl appropriately illustrates the application of his model by a consideration of the nodal properties of the HOMO and LUMO orbitals of an appropriate parent annulene, e.g., $C_{16}H_{16}^{2-}$. He then considers the effects on its energy levels of distorting the shape of the regular polygon to one having D_{4h} symmetry, the effect of the interaction with four ethylene units, and the effect of the four aza replacements. Next, the HOMO and LUMO energy levels of the resulting porphine dianion are modified to those of the reduced porphyrins on the basis of qualitative PMO[12] type arguments. Finally, the relative absolute sizes of the ΔHOMO's and ΔLUMO's are used to predict the absolute signs of the MCD bands.

In an alternative approach we require a protocol which retains the intuitive accessibility of Michl's parent perimeter treatment but which also provides a way of estimating orbital-energy changes on the basis of experimental data. The first requirement is served nicely by returning to the classic four-orbital model of Gouterman[11] wherein he melded the concepts of the cyclic polyene model for porphyrins with those generated by early LCAO-MO calculations.[25] In this model the LUMO's are degenerate by symmetry

(16) Petke, J. D.; Maggiora, G. M.; Shipman, L. L.; Christoffersen, R. E. *J. Mol. Spectrosc.* **1978**, *73*, 311–331.
(17) Petke, J. D.; Maggiora, G. M.; Shipman, L. L.; Christoffersen, R. E. *J. Mol. Spectrosc.* **1978**, *71*, 64–84.
(18) Nordén, B.; Davidson, A. *Chem. Phys. Lett.* **1976**, *37*, 433–437.
(19) (a) Gale, R.; Peacock, R. D.; Samori, B. *Chem. Phys. Lett.* **1976**, *37*, 430–433. (b) Fischer, N.; Goldammer, E. V.; Pelzl, J. *J. Mol. Struct.* **1979**, *56*, 95–105.
(20) Castellan, A.; Michl, J. *J. Am. Chem. Soc.* **1978**, *100*, 6824–6827.
(21) Vašák, M.; Whipple, M. R.; Michl, J. *J. Am. Chem. Soc.* **1978**, *100*, 6838–6843.
(22) Petke, J. D.; Maggiora, G. M.; Shipman, L. L.; Christoffersen, R. E. *Photochem. Photobiol.* **1980**, *32*, 399–414.
(23) Weiss, C. Jr. *J. Mol. Spectrosc.* **1972**, *44*, 37–80.
(24) Gale, R.; McCaffery, A. J.; Rowe, M. D. *J. Chem. Soc., Dalton Trans.* **1972**, 596–604.

Table II. Ratios of Visible Absorption Band Maxima of Symmetric Porphyrins

porphyrin derivative	$\epsilon_{max}(Q_0)/\epsilon_{max}(Q_1)$	$\lambda_{max}(Q_0)$, nm
porphine		
dianion	0.06	584[c]
dication	0.16[a]	585[c]
zinc	0.44	560
zinc pyridine	0.13	569
octaethylporphyrin		
dianion	0.49	588
dication	0.47	592
zinc	1.83	568
zinc pyridine	0.87	578
tetraphenylporphyrin		
dianion	0.99	621
dication	5.66[b]	655
zinc	0.16	590
zinc pyridine	0.47	601

[a] Probably overestimated since the Q_0 band is observed only as a broad shoulder on the Q_1 band. [b] Anomalously high value; excluded from consideration in the data base, see ref 28. [c] MCD *A*-term crossover.

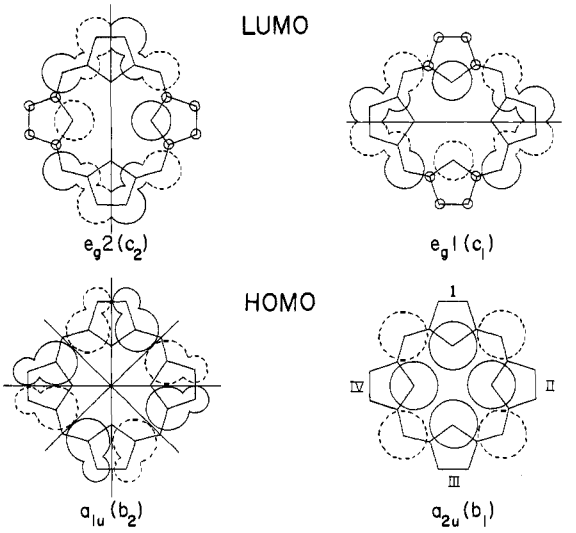

Figure 2. Porphin HOMO and LUMO orbitals redrawn from ref 11a. The sizes of the circles are proportional to the atomic orbital coefficients of Seely.[25] Symmetry nodes are indicated by lines. The labels e_g1, e_g2, a_{2u}, a_{1u} are appropriate for D_{4h} porphyrins, whereas the labels c_1, c_2, b_1, b_2 are used to indicate their descendents in porphyrin derivatives of lower symmetry.

and the HOMO's are assumed to be accidentally so. Interaction between the degenerate singly excited configurations then gives rise to pairs of degenerate states which are identified with the strong Soret and the weak visible transitions of symmetric porphyrins. In the event that the HOMO degeneracy is exact, the Q_0 transition vanishes and a reference point is reached which is analogous to the one guaranteed by symmetry for the $C_{16}H_{16}^{2-}$ polyene (Figure 1a). The data collected in Table II for the ratios of the intensities of the visible bands of some porphyrins, $\epsilon_{max}(Q_0)/\epsilon_{max}(Q_1)$,[26] indicate that the condition of $\Delta HOMO = \Delta LUMO = 0$ is very closely approximated in the case of porphine dianion and possibly in porphine dication as well. Thus, porphine dianion, in particular, can be used as a suitable reference porphyrin

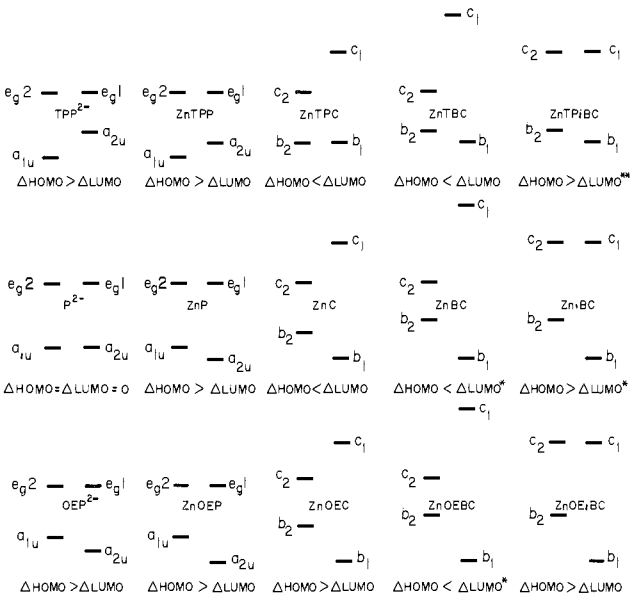

Figure 3. Orbital energy level diagrams adduced for zinc porphyrins, chlorins, bacteriochlorins, and isobacteriochlorins with use of the protocol developed in the text. The single asterisk denotes predictions not yet confirmed by experiment. The double asterisk indicates a prediction that is inconsistent with experimental results. The source of the inconsistency is discussed in the text.

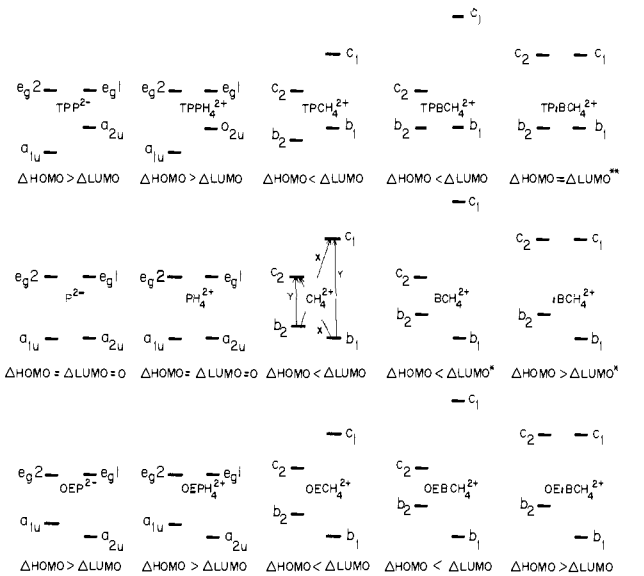

Figure 4. Orbital energy level diagrams adduced for the porphyrin, chlorin, bacteriochlorin, and isobacteriochlorin dications with use of the protocol developed in the text. The meaning of the single and double asterisks is given in the legend to Figure 3. ΔHOMO for tetraphenylporphyrin dication is not scaled to reflect the absorption band ratio given in Table II for the reason noted in ref 28.

in a perturbation treatment. Another advantage of the direct implementation of the four-orbital concept is that Gouterman's representation[11a] of Seely's[25] AO coefficients for porphin shown in Figure 2 can be used to provide a visual way of estimating the relative magnitudes of the effects of substituents on the energy levels of the HOMO and LUMO orbitals. PMO considerations regarding the relative position of the substituent LUMO or HOMO with respect to those of the porphyrin substrate can also be incorporated.[7c,12]

The requirement of an experimental basis for calibrating orbital energy level changes is fulfilled by the data collected in Table II. These data, in conjunction with knowledge of the orbitals most affected by the substituent as derived from Figure 2, permit the ordering and relative splitting of the HOMO's of the symmetrically

(25) Seely, G. R. *J. Chem. Phys.* **1957**, *27*, 125–133.

(26) We use this ratio as a measure of the degeneracy of the HOMO's of symmetric porphyrins rather than that of $\epsilon_{max}Q_0/\epsilon_{max}$ Soret since data for the latter for porphine dianion are not available (ref 13). Its usage is justified by Spellane et al.[27] on the basis that the intensity of the Q_1 transition is due to vibronic mixing of the Q state with the Soret state and is relatively constant for a variety of symmetric porphyrins.

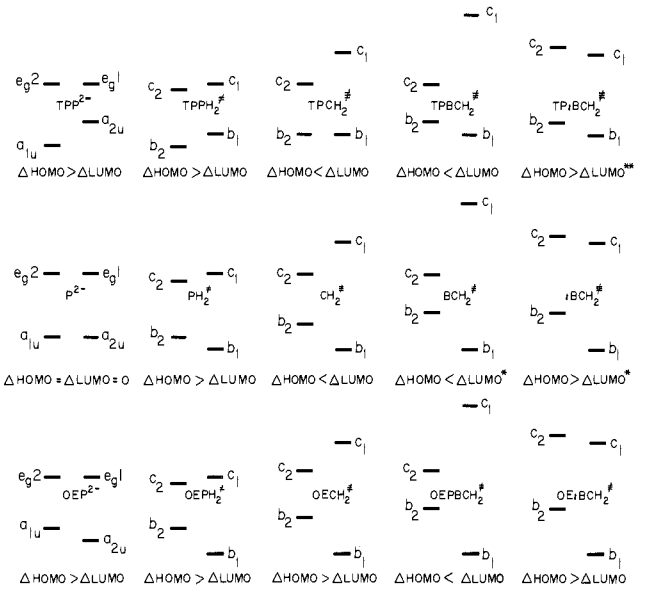

Figure 5. Orbital energy level diagrams adduced for the free-base porphyrins, chlorins, bacteriochlorins, and isobacteriochlorins with use of the protocol developed in the text. Single and double asterisks have the meanings given in the legend to Figure 3. The symbol $\neq$ indicates that the hydrogens are placed on the x axis, whereas the symbol $\not\equiv$ indicates that they lie on the y axis.

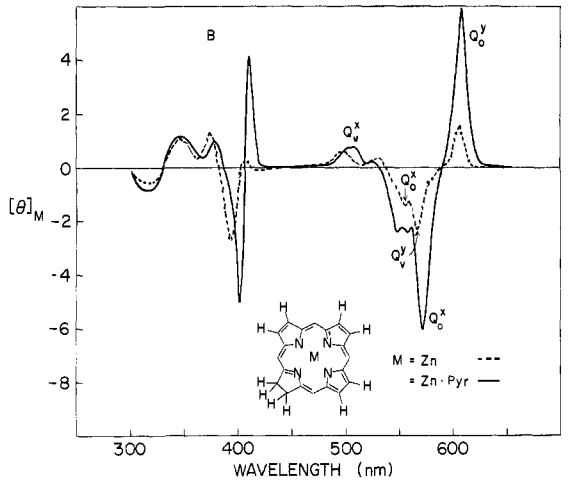

Figure 6. MCD spectra of zinc chlorin in benzene (---) and in pyridine (—).

substituted porphyrins to be estimated. These changes are then coupled with a separate experimentally derived estimate for the effects of the "chlorin" perturbation on both the HOMO's and LUMO's to generate the energy-level diagrams for the zinc (Figure 3), dication (Figure 4), and free-base (Figure 5) derivatives of the reduced porphyrins. Some additional considerations needed for isobacteriochlorins are introduced in Figure 9. MCD data for the dianions are available only for the chlorins and porphyrins (Table I) and consequently they are not explicitly incorporated in the diagrams for the reduced series. The changes in the MCD of the zinc complexes of the chlorins on ligation with pyridine are of particular interest with regard to the soft MCD chromophore case, i.e., where $\Delta HOMO = \Delta LUMO \neq 0$, and they are considered explicitly by reference to the experimental spectra shown in Figures 6–8. The final step of the procedure is to use the so estimated relative magnitudes of $\Delta HOMO$ and $\Delta LUMO$ along with Michl's predictions of the expected MCD band sign patterns, as summarized in Figure 1, to deduce the sign patterns for the substituted reduced porphyrins.

In order to make our conclusions about the effects of substituents on the energy levels of the frontier MO's of porphine dianion more explicit, we turn first to a consideration of totally symmetric

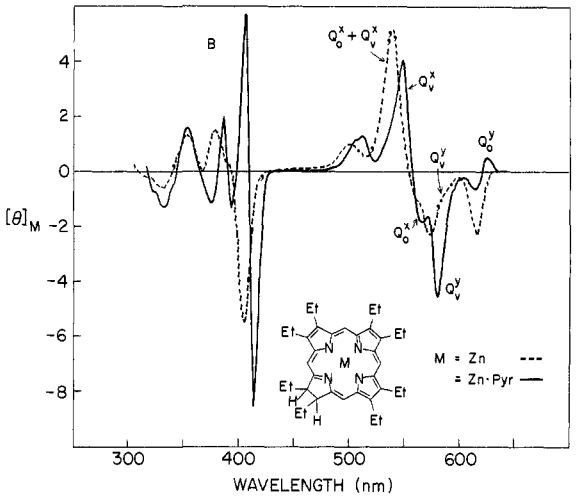

Figure 7. MCD spectra of zinc octaethylchlorin in benzene (---) and in pyridine (—).

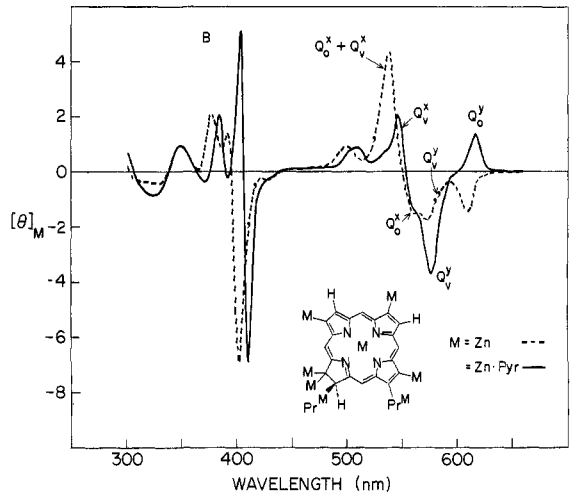

Figure 8. MCD spectra of zinc bonellin in benzene (---) and in pyridine (—).

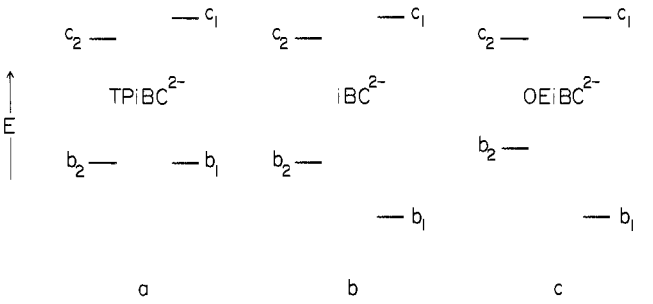

Figure 9. Orbital energy level diagrams for the (a) tetraphenylchlorin, (b) unsubstituted chlorin, and (c) octaethylisobacteriochlorin dianions which incorporate the split in the LUMO's which obtain from explicit MO calculations.

perturbations and note that they have identical effects on both LUMO's. Consequently, these changes are not scaled in the diagrams of Figures 3–5. The nodal properties of the HOMO orbitals given in Figure 2 show that the a_{1u} orbital has nodes through the nitrogen atoms; consequently, a central substituent such as zinc can only affect the energy level of the a_{2u} orbital. Conjugation of the π orbital of the metal with those of the porphyrin ring results in electron withdrawal from the ring. As a consequence the a_{2u} orbital of zinc porphine is lowered in comparison to porphine dianion. The scaling adopted for this orbital-energy change in the diagram for zinc porphine shown in Figure 3 is indexed to the increase in the ratio of the visible

absorption band intensities of the two compounds which are given in Table II. Insertion of four protons to generate the dication also lowers the energy of the a_{2u} orbital; however, the mechanism is an inductive rather than a mesomeric one. The change should thus be much smaller as is suggested by the value of the ratio tabulated for porphine dication in Table II. This shift is not scaled in the diagram given for porphine dication in Figure 4 and we consider that for it, as for porphine dianion, $\Delta HOMO \approx 0$. With regard to the effects of pyridine ligation, we assume along with Nappa and Valentine[29] and with Spellane et al.[27] that, within the context of the concepts of the four-orbital model, complexation with donor ligands can be simply regarded as causing an increased transfer of electron density through the metal onto the ring. This increase in electron density in the a_{2u} orbital should result in a rise in its energy with the consequence that the separation between the energy levels of the HOMO's of the pyridinate complex of zinc porphine should be smaller than that in the unligated species. The decrease in the visible absorption band ratio from 0.44 to 0.13 and the red shift in the position of the Q_0 band (Table II) are both consistent with the proposed energy-level shift.

There is some uncertainty in the literature about whether meso phenyl groups are electron-donating or electron-withdrawing substituents and whether their effect should be considered as inductive, mesomeric, or a combination of the two. For example, in their CNDO/2 and CNDO/S calculations on tetraphenylporphyrin, Chantrell et al.[30] considered only the perpendicular conformation for the phenyl rings and concluded that they withdraw electron density. A body of evidence, however, suggests that there is considerable π delocalization between the phenyl and the porphyrin rings.[27,31-34] The work of Moet-Ner and Adler[33] indicates that the mesomeric effect dominates. According to PMO theory[12] phenyl groups are $\pm E$ substituents. As such, they lower the energy levels of the LUMO's but raise those of the HOMO's. For porphyrins, both LUMO orbitals shift by the same amount and so, again, these changes are not scaled in the energy-level diagrams of Figures 3-5. In the HOMO's only the a_{2u} orbital has electron density at the meso positions and the phenyl substituents should cause its energy to rise. The large increase in the absorption band ratio from 0.06 to about 1 on going from porphine dianion to tetraphenylporphyrin dianion (Table II) is reflected in the spacing scaled for the separation between its a_{1u} and a_{2u} orbitals given in Figures 3-5. Substitution of zinc into the core of tetraphenylporphyrin dianion should, because of electron withdrawal by the metal, lower the energy of the a_{2u} orbital. This orbital-energy shift should be, and is, accompanied by a decrease in the absorption band ratio and by a blue shift in the position of the Q_0 band. Pyridine ligation counterbalances some of the electron withdrawal due to zinc. The absorption band ratio again increases and the Q_0 band red shifts.

Alkyl groups donate electron density to the porphyrin ring[11] and can be considered as weak $-E$ substituents.[35] Their symmetric substitution on the porphyrin ring leaves the relative positions of the LUMO orbitals unchanged. Since the a_{2u} orbital has little electron density on the pyrrole carbons (Figure 2), the dominant effect of the substitution of eight alkyl groups should be to raise the energy of the a_{1u} orbital. The rise in the energy of the a_{1u} orbital owing to alkyl substitution is smaller than the rise in the a_{2u} HOMO on phenyl substitution since the visible absorption band ratio only increases from 0.06 to 0.49 on going from porphine dianion to octaethylporphyrin dianion (Table II). This accounts for the factor of 2 difference in the scaling of the a_{1u}, a_{2u} energy-level separations for the octaethyl- and tetraphenylporphyrin dianions in Figure 3-5. For octaethylporphyrin dianion insertion of zinc and its subsequent ligation by pyridine alters the energy of the a_{2u} orbital, thereby resulting in absorption band ratio changes and wavelength shifts which parallel those already noted for the unsubstituted porphine.

Symmetry-lowering perturbations in the present series are of two kinds. In the first, two protons are inserted into the core of the dianion to form the free-base porphyrin. In the second, one or more pyrrole ring double bonds are removed from the π system by chemical reduction to form the chlorins or the two tetrahydro derivatives, the bacteriochlorins, and the isobacteriochlorins. Both perturbations lead to separations in the energy levels of the HOMO orbitals as well as in those of the LUMO's. In accordance with the convention adopted for the proton axis for the free-base porphyrins which was specified in Figure 1 of Part 1[1] and which is again noted here in the legend to Figure 5, addition of the two inductively electron withdrawing protons to the core of porphine dianion should result in a lowering of the energies of its e_g2 and a_{2u} orbitals.[11a] The energies of the e_g1 and a_{1u} orbitals are not affected because of their nodal properties. Two considerations contribute to the scaling adopted in Figure 5 for the relative energy separation between the c_1 and c_2 (LUMO) orbitals (see ref 36) and between the b_1 and b_2 (HOMO) orbitals of porphine. First, note in Figure 2 that the orbital coefficients at the nitrogens in the affected LUMO (e_g2) of the reference porphyrin, porphine dianion, are smaller than those in the HOMO (a_{2u}). Consequently, on this basis alone one would expect that $\Delta HOMO > \Delta LUMO$ for free-base porphine. Second, this condition of inequality is consistent with the tenets of Michl's model since porphine exhibits (Figure 2, Part 1[1]) the normal (−+−+) MCD band sign pattern for its visible and Soret transitions. Notice also in Figure 5 that the scaling of the HOMO separation for the three free-base porphyrins is in the order $PH_2 \approx TPPH_2 < OEPH_2$. This ordering is determined by the scaling assessed from the absorption spectra of the dianions for the effects of symmetric alkyl and phenyl substitution. This ordering is also consistent with the ordering of the visible absorption band ratios $(\epsilon_{max}(Q_0^x) + \epsilon_{max}(Q_0^y))/(\epsilon_{max}(Q_1^x) + \epsilon_{max}(Q_1^y))$ for PH_2, $TPPH_2$, and $OEPH_2$ of 0.17, 0.43, and 0.78, respectively, given by Spellane et al.[27] Finally, it should be noted that this scaling for the free-base perturbation is carried over to the reduced porphyrins. However, since the proton axis for the reduced porphyrins differs from that of the free-base porphyrins (legend to Figure 5), a different LUMO will be affected by the protons.

Several criteria can be used to establish the relative orbital-energy shifts which attend the "chlorin" perturbation. First, we note that the chlorin perturbation can be viewed[11a,37] as reducing the size of the π systems of the orbitals affected. According to our axis convention (Figure 1, Part 1[1]), protons are placed on the pyrrole carbons of ring IV (Figure 2). Consequently, the a_{1u} and e_g1 orbitals of porphine dianion should rise in energy on going to chlorin dianion. In a preliminary communication (ref 1, Part 1[1]), we counted the increase in energy for e_g1 as being greater than that for a_{1u} since the electron density at the site of reduction is larger in the former than in the latter orbital and noted that the e_g2 and a_{2u} orbitals remain relatively unaffected. While this argument is consistent with results from MO calculations,[11] the reader may be more satisfied by Michl's[7b] PMO treatment which starts from the perimeter MO's. The shifts expected for chlorin dianion are graphically illustrated for chlorin dication (porphine dication also serves, as already noted, as a reference porphyrin) in Figure 4. A rough experimental estimate of the relative magnitudes of $\Delta HOMO$ and $\Delta LUMO$ for chlorin dianion, or

(27) Spellane, P. J.; Gouterman, M.; Antipas, A.; Kim, S.; Lu, Y. C. *Inorg. Chem.* **1980**, *19*, 386-391.

(28) (a) Stone, A.; Fleischer, E. B. *J. Am. Chem. Soc.* **1968**, *90*, 2735-2748. (b) Dirks, J. W.; Underwood, G.; Matheson, J. C.; Gust, D. *J. Org. Chem.* **1979**, *44*, 2551-2555. $TPPH_4^{2+}$ is markedly nonplanar, S_4 conformation, in the solid state and probably in solution as well. The LUMO's are still degenerate by symmetry. The narrower angle of about 21° between the mean plane of the porphyrin ring and those of the phenyl group as compared to most metal tetraphenylporphyrins (~90°) should result in enhanced overlap of the π systems which could lead to a large splitting in the HOMO's, thereby accounting for the anomalously large ratio of visible absorption band intensities given in Table II.

(29) Nappa, M.; Valentine, J. S. *J. Am. Chem. Soc.* **1978**, *100*, 5075-5080.

(30) Chantrell, S. J.; McAuliffe, C. A.; Munn, R. W.; Pratt, A. C.; Weaver, R. F. *Bioinorg. Chem.* **1977**, *7*, 283-296.

(31) Fuschsman, W. H.; Smith, Q. R.; Stein, M. M. *J. Am. Chem. Soc.* **1977**, *99*, 4190-4192.

(32) Eaton, S. S.; Eaton, G. R. *J. Am. Chem. Soc.* **1975**, *97*, 3660-3666.

(33) Moet-Ner, M.; Adler, A. D. *J. Am. Chem. Soc.* **1975**, *97*, 5107-5111.

(34) Wolberg, A. *J. Mol. Struct.* **1974**, *21*, 61-66.

(35) Whipple, M. R.; Vasak, M.; Michl, J. *J. Am. Chem. Soc.* **1978**, *100*, 6844-6852.

chlorin dication, comes from the four-orbital concept[11] that since the Q_0^x transition of chlorins is always very weak compared to the Q_0^y transition, the x-polarized states must be nearly degenerate as is indicated in Figure 4. As a last criterion, we note that while it is very difficult to derive from absorption spectral data alone a more quantitative estimate of the orbital-energy shifts attending the chlorin perturbation because of the extreme weakness of the Q_0^x transition and its interdigitation with vibronic bands, the scaling for the separate HOMO and LUMO energy-level shifts must be consistent with the fact that rather subtle substituent effects do result in the sign variations summarized in Table I. Finally, we note that in the tetrahydro series the second chlorin perturbation is weighted the same as the first. In the bacteriochlorins two chlorin perturbations cause a rise in the energy of the c_1 orbital, a result which is consistent with findings from MO calculations.[11] In the isobacteriochlorins both the c_1 and c_2 orbitals undergo the rise in energy and it will be necessary in the pertinent section to include, in an ad hoc manner, the LUMO splitting which comes out of MO calculations.

It may be useful to conclude this section with a brief summary of the elements which form the basis of our protocol and to add some codas about its implementation as discussed in the next section. (i) Orbital-energy changes are viewed in the context of the classical four-orbital model of Goutermann[11] and the shifts are calibrated on the basis of experimental spectral data. (ii) The symmetrical (i.e., phenyl, alkyl, dication, zinc, and zinc pyridinate) perturbations set the shifts in the HOMO energy levels but cause no relative changes in those of the LUMO's. (iii) The free-base perturbation results in relative changes in both the HOMO and LUMO energy levels for which experimentally determined limits can be set. These shifts can be regarded as independent of the effects of the alkyl and phenyl groups. (iv) The experimentally evaluated chlorin perturbation also causes relative shifts in the energy levels of both the HOMO's and LUMO's which can be taken as additive to the free-base perturbation and to those of the totally symmetric perturbers with the exception of that of the alkyl groups. For them, the chlorin perturbation removes the effects of two or more of the alkyl groups. Consequently, the procedure of first applying the totally symmetric alkyl perturbation to porphine dianion and then introducing the chlorin perturbation in order to generate the energy-level diagram of, for example, octaethylchlorin dianion does not have strict validity within the model elaborated above. (v) To allow for the explicit recognition of the variable contribution of the alkyl perturbers in the generation of the energy-level diagrams for the alkyl-substituted reduced porphyrins (Figures 3–5), we recall first that their effect is a relatively small one as judged by the absorption spectral changes on going from porphine dianion to octaethylporphyrin dianion (Table II). Second, we note that the perturbation protocol should be internally self-consistent. This is to say that one should be able to proceed from porphine dianion to chlorin dianion to octaethylchlorin dianion. This latter perturbation route is, however, difficult to calibrate on the basis of absorption spectral changes alone but is accessible by the application of PMO[12] arguments such as those set down by Michl.[7c] For this purpose we turn to the representations of the AO coefficients of the porphin MO's given in Figure 2 and consider the results of conjunctive application of the chlorin and alkyl perturbations. For the a_{1u} HOMO only six alkyl groups are effective in contributing to its rise in energy, whereas either two or four alkyl groups must be counted for the e_g1 and e_g2 orbitals, respectively. Since the alkyl donor orbitals are closer in energy to the HOMO's than to the LUMO's of the porphine substrate, we take their effects on the energy levels of the former (a_{1u}) to be greater than on the latter (e_g1 and e_g2). As noted above, the alkyl effect is a small one; however, we accommodate in Figures 3–5 the above considerations by a proportionate decrease in the extent to which the HOMO and LUMO energy levels are increased owing to alkyl substitution.

As a final comment we note that while the attributes of the protocol just outlined are its experimental basis and its intuitive accessibility, it may be possible to evaluate the effects of the perturbations considered above on a more quantitative basis. The approach is basically the one used by Gouterman[38] in his initial paper on porphyrin-substituent effects. Essentially, it requires parametrization of substituent effects in terms of the symmetries of the perturbations that mix the Q and B states of porphyrins. This requires a detailed numerical analysis of both absorption and MCD data but does lead to quantitative predictions for the *B* terms and dipole strengths of the Q_0^x and Q_0^y transitions of substituted reduced porphyrins.[39] In the present paper we focus our attention almost entirely on the signs rather than the magnitudes of the MCD bands.

Structure–Spectra Correlations. In the preceding section we gave a detailed exposition of the protocol for generating the diagrams in Figures 3–5, placing particular emphasis on the way in which experimental spectral data were used to scale the relative changes in the orbital-energy levels. In this section it will be economical to center the discussion more heavily around simple notions of perturbation theory. Predicted MCD band sign patterns are implcitly given by the inequality relations in Figures 3–5 and explicitly given in Table I where they are directly compared with experiment. Emphasis is placed on the MCD band sign patterns (either normal, $-+-+$, or inverted, $+-+-$) governed by μ^+ contributions; however, the possibility that these may be overlaid by the $---+$ pattern arising from μ^- contributions is considered for cases where the condition $\Delta\text{HOMO} \approx \Delta\text{LUMO}$ may be supposed to exist. For reasons stated in an earlier section, the μ^- contributions to the lowest-energy, Q_0^x and Q_0^y, MCD bands are expected to be very small and we will be primarily concerned, where needed, with the stronger μ^- imposed $-+$ pattern in the Soret region. In Table I the μ^+ pattern is given in brackets for both the visible and Soret bands. The μ^- pattern is placed in parentheses. Incorrect predictions for the signs of the MCD Q bands which arise from direct application of the protocol are signaled by a double asterisk in Figures 3–5. These predictions for isobacteriochlorins are included in Table I in the usual square brackets. The amended predictions for them which arise when the LUMO splitting is included in the protocol are given in braces. The section concludes with a consideration of how the model can be applied to other substituted reduced porphyrins.

(i) **Porphyrins.** Symmetric substitution at the periphery of porphine dianion or porphine dication forces a splitting of the originally accidentally degenerate HOMO's as shown in Figures 3–5. In the case of meso phenyl substitution the a_{2u} orbital rises in energy, whereas for octaalkyl substitution at the pyrrole carbons it is the a_{1u} orbital that rises. Further substituion at the porphyrin core, e.g., H_4^{2+}, Zn, or Zn-Pyr, serves primarily to modulate the separation between these orbitals. For these porphyrins $\Delta\text{HOMO} > \Delta\text{LUMO}$, and Michl's prediction[7a] of the normal MCD band sign for both the Soret and visible electronic transitions is confirmed as is indicated in Table I. In the event that particular symmetrical substituents, e.g., *meso*-pentafluorophenyl,[15] result in near degeneracy of the HOMO's, the sign pattern in the Q_0 band may be inverted just as it is for porphine dianion and dication.[13,14]

Unsymmetrical substitution on the porphine chromophore such as that leading to the free-base porphyrins results in the splitting of both the HOMO's and LUMO's. According to our attribution in the preceding section of protons as inductive electron-withdrawing substituents, their placement on the pyrrole nitrogens along the x axis of porphine dianion should result in the lowering of the e_g2 and a_{2u} orbitals with the larger change being effected in the HOMO because of the relative difference in the size of the AO coefficients (Figure 2) for this orbital at the points of attachment as compared to those in the affected LUMO. The condition $\Delta\text{HOMO} > \Delta\text{LUMO}$ shown for free-base porphine in

(36) The orbital symmetry labels a_{1u}, a_{2u}, and $e_g1,2$ are not appropriate for unsymmetrical porphyrin derivatives. We adopt Gouterman's usage[11a] and take c_1, c_2, b_1, and b_2 to be descendents of the unperturbed e_g1, e_g2, a_{2u}, and a_{1u} orbitals, respectively, throughout the series.

(37) Spangler, D.; Maggiora, G. M.; Shipman, L. L.; Christoffersen, R. E. *J. Am. Chem. Soc.* **1977**, *99*, 7470–7477.

(38) Gouterman, M. *J. Chem. Phys.* **1959**, *30*, 1139–1161.

(39) Keegan, J. D. Ph.D. Thesis, Stanford University, 1981.

Figure 5 leads to the prediction, according to Michl's model,[7b] of a normal MCD band sign pattern for the Soret and visible electronic transitions which is confirmed by experiment (Table I, also Figure 2 of Part 1[1]). For the phenyl- and alkyl-substituted series the effects of the free-base perturbation are best viewed by applying the totally symmetric perturbation first. Conversion of porphine dianion to tetraphenylporphyrin dianion is attended by a large increase in the energy of the a_{2u} orbital. Application of the free-base perturbation results in the split in the LUMO's shown for tetraphenylporphyrin in Figure 5 and in a lowering in the energy level of the descendant of the a_{2u} orbital, the b_1 orbital. However, the condition of $\Delta HOMO > \Delta LUMO$ is maintained and the normal sign pattern predicted for tetraphenylporphyrin free base is the one observed experimentally (Table I). For alkyl-substituted free-base porphyrins the condition $\Delta HOMO > \Delta LUMO$ is guaranteed since the eight pyrrole alkyl groups initially raised the a_{1u} orbital and the free-base perturbation only serves to widen the split in the HOMO's. It is important to notice, however, that the spacing depicted for the splitting of the HOMO's and LUMO's for free-base porphine in Figure 5 suggests that the potential exists for a perimeter symmetric perturbation in free-base porphyrins such that the condition $\Delta HOMO < \Delta LUMO$ obtains. While the consequent inverted pattern has been observed in a few special cases, e.g., in the Q_0^x and Q_0^y MCD bands of tetrakis-(pentafluorophenyl)porphyrin,[15] one can safely predict that D_{2h} porphyrin free bases will commonly exhibit the normal $-+-+$ MCD band sign pattern.

(ii) Chlorins. A similar possibility for substituent-induced MCD band sign variation, i.e., cases where, within a series of closely related compounds, the condition $\Delta HOMO > \Delta LUMO$ or else $\Delta HOMO < \Delta LUMO$ may obtain, is also suggested by the diagrams for the unsubstituted chlorins shown in Figures 3–5. In arriving at the energy-level diagram for chlorin dianion (which is taken to be the same as that shown for chlorin dication in Figure 4) we used the argument that the decrease in the size of the conjugation path in the a_{1u} HOMO and in the e_g1 LUMO of porphine dianion attending reduction of the pyrrole double bond in ring IV was responsible for their rise in energy and that the rise in the latter was larger than that in the former. Thus, for chlorin dianion or chlorin dication $\Delta HOMO < \Delta LUMO$ and the consequent prediction of an inverted MCD band sign pattern for them is confirmed by experiment with certainty for the Q bands. There is some uncertainty, as indicated in Table I, for the Soret band of chlorin dianion; however, the Soret MCD bands of chlorin dication are clearly inverted as expected. Insertion of zinc into the core of chlorin dianion has the effect of lowering the energy of the b_1 orbital thereby widening the gap between the HOMO energy levels. Ligation with pyridine again raises the level of the b_1 orbital and the HOMO split decreases. For both bare and ligated zinc chlorin we predict $\Delta HOMO < \Delta LUMO$ and an inverted pattern in its MCD bands. This is the pattern observed for the visible as well as the Soret MCD bands of the pyridinate complex (Figure 6). The visible bands of the unligated zinc complex are also inverted as shown in Figure 6; however, congruence with the prediction based on dominance of the μ^+ contribution for the Soret region can only be obtained if the small positive band at 408 nm is taken as the lowest-energy Soret MCD band. This is not an unreasonable assumption (a similar one is required for chlorin dianion) on the basis of the way in which oppositely signed MCD bands may overlap to produce the observed experimental band shape. However, we note that the selection of the stronger bands as being the main four-orbital transitions suggests that for chlorin dianion and zinc chlorin the condition of $\Delta HOMO \approx \Delta LUMO$ is being approached and that one must consider that the invariant μ^- sign pattern of $-+$ dominates in contributing to the signs of the Soret MCD bands for these chlorin derivatives. Further support for the idea that the condition of near equality in the splitting of the HOMO's and LUMO's is being broached in the unsubstituted chlorin series is gained from a consideration of the energy-level diagram and the MCD spectrum of free-base chlorin. For chlorin free bases, in contrast to the usual practice for porphyrins, protons are placed on the pyrrole nitrogens which lie on the y axis. As a consequence, the c_1 and b_1 orbitals of chlorin dianion (see chlorin dication in Figure 4) are both lowered thereby leading to the nearly equal HOMO and LUMO orbital separations depicted for chlorin in Figure 5. That the condition $\Delta HOMO < \Delta HOMO$ is maintained is evidenced by the inverted pattern observed for the Q bands of chlorin as shown in Figure 3 of Part 1. However, the two lowest-energy Soret MCD bands now unequivocally exhibit the normal $-+$ sign pattern. Within the context of Michl's model[7a,b] this situation can only occur when the μ^- contributions attending the condition of near equality between $\Delta HOMO$ and $\Delta LUMO$ dominate μ^+ contributions in the higher-energy bands and thus determine the signs of the Soret bands. For the Q bands, on the other hand, the μ^+ contribution dominates the much weaker μ^- contribution.

In the tetraphenylchlorin series the net effect of the conjunctive application of the phenyl and chlorin perturbations to the MO's of porphine dianion is to introduce a large split in the LUMO's but a much smaller one in the HOMO's. This can be readily seen by the reader upon comparison of the orbital energy level diagrams for the corresponding centrally substituted derivatives of chlorin and tetraphenylchlorin in Figures 3–5. As an example, notice in Figure 3 that the application of the tetraphenyl perturbation to zinc chlorin results in a significant increase in the energy of the b_1 orbital. The consequence is that the rise in the b_2 orbital which accompanied the chlorin perturbation (i.e., ZnP → ZnC) is now balanced by the rise of the b_1 orbital and according to our experimentally based scaling considerations the HOMO's of zinc tetraphenylchlorin become accidentally degenerate. The resulting condition that $\Delta HOMO < \Delta LUMO$ is found to varying extents throughout the tetraphenylchlorin series. Furthermore, since the quantity $|\Delta HOMO - \Delta LUMO|$ is predicted to be relatively large, one should reasonably expect μ^+ contributions to dominate and to determine the signs of the MCD bands of both the Soret and visible transitions. This expectation of the inverted $+-+-$ pattern is indeed matched by the experimental data (Table I) for the tetraphenylchlorin series *except* for tetraphenylchlorin free base for which the Soret MCD bands have the normal sign pattern of $-+$. According to the energy-level diagram given in Figure 5, $\Delta HOMO \approx 0$ for tetraphenylchlorin. The correlation of the condition of near equality between $\Delta HOMO$ and $\Delta LUMO$ and the consequent contribution of the μ^- Soret MCD band sign pattern of $-+$ invoked with good reason for chlorin free base (vide supra) does not seem to obtain for tetraphenylchlorin. A discrepancy of this kind indicates that the Soret transitions are not well described by a four-orbital model.

In the alkyl-substituted chlorins the effect of the alkyl perturbers is to force the condition of near equality between the $\Delta HOMO$'s and $\Delta LUMO$'s even more closely than is the case in the unsubstituted series. The consequence of the quantity $|\Delta HOMO - \Delta LUMO|$ becoming small is that the sign of $\Delta HOMO - \Delta LUMO$ may vary, depending on the particular central substituent or on the details of the peripheral substitution. As an example, consider the chlorin dications whose orbital energy level diagrams are given in Figure 4. Application of the chlorin perturbation to porphine dication raises the energies of its e_g1 and a_{1u} orbitals. $\Delta HOMO < \Delta LUMO$ and the magnitude of the quantity $|\Delta HOMO - \Delta LUMO|$ is judged to be relatively large. The μ^+ moment contributions should dominate and determine the sign pattern of the MCD bands. Table I shows that indeed the prediction for chlorin dication agrees with the experimental observation of the inverted pattern in both the Soret and Q transitions. Starting with chlorin dication as our basis we now apply the alkyl perturbation as specified in the preceding section. Six alkyl groups are effective (because of the chlorin perturbation) in raising the energy of the b_2 orbital, whereas only four and two alkyl groups are counted as effective in raising the energies of the c_2 and c_1 LUMO's, respectively. The weighting of the energy shifts per alkyl group is greater for the HOMO than for the LUMO's; however, the condition of $\Delta HOMO < \Delta LUMO$ is maintained and the sign pattern predicted for octaethylchlorin dication on the basis of only the μ^+ contribution is the inverted one, $+-+-$, which is in accord with experiment (Table I). For zinc octaethylchlorin a different

balance in the relative energy-level distribution of the HOMO's and LUMO's is reached because of the mesomeric electron-withdrawing character of zinc. Starting with porphine dianion, insertion of zinc is accompanied by a lowering of the energy level of the a_{2u} orbital to the position shown for zinc porphine in Figure 3. Application of the standard chlorin energy-level shifts results in the condition $\Delta HOMO < \Delta LUMO$ shown for zinc chlorin and the prediction of the inverted MCD band sign pattern (Table I). Again, as in the case of the dication considered above, six alkyl groups are counted as effecting the rise in the b_2 orbital but only four and two alkyl groups are effective in increasing the energy of the c_2 and c_1 LUMO's, respectively. However, now, because of the initial lowering of the b_1 orbital by zinc, the resultant splitting in the HOMO is greater than that in the LUMO, and we predict that zinc octaethylchlorin should exhibit the normal $-+-+$ MCD band sign pattern for its Soret and visible transitions. The data in Table I and the spectrum of zinc octaethylchlorin shown in Figure 7 are consistent with this prediction. In this case, the quantity $|\Delta HOMO - \Delta LUMO|$ is again small and the MCD band sign pattern in the Q bands $(-+)$ is determined by the μ^+ moment contributions. In the Soret region the sign patterns determined by the μ^+ and μ^- moments are the same $(-+)$ and so reinforce each other. Recall, however, that in the case of zinc chlorin where $|\Delta HOMO - \Delta LUMO|$ was also small, the μ^+ moment won out in the Q bands, giving the inverted pattern, but the μ^- contribution swamped the μ^+ contribution in the Soret bands and led to the normal pattern.

Further insight into the distribution of orbital-energy levels that may exist for soft or almost soft MCD chromophores can be gained by considering orbital shifts arising from the formation of the zinc pyridinate complexes. As already discussed, the effect of ligation in the case of zinc chlorin is to raise the energy level of the b_1 orbital (Figure 3), thereby enforcing the condition that $\Delta HOMO < \Delta LUMO$. In the MCD spectrum (Figure 6) this is attended by an increase in the intensities of the visible and Soret MCD bands, and the inverted MCD band pattern observed in both regions is unequivocally the one expected for the μ^+ contribution. On the other hand, in the case of zinc octaethylchlorin the effect of ligation with pyridine is again to raise the level of the b_1 orbital but now, since initially $\Delta HOMO > \Delta LUMO$ for the unligated species, the result is to narrow the separation between the HOMO's and $\Delta HOMO$ becomes very nearly equal in magnitude to $\Delta LUMO$. In the MCD spectrum of the pyridinate complex of zinc octaethylchlorin shown in Figure 7, the MCD associated with the Q_0^y transition becomes small and takes on a mixed sign pattern, the MCD associated with the Q_0^x transition is observed as the negative band at 566 nm, and the Soret region MCD bands assume a well defined $-+$ sign pattern. We believe that the condition $\Delta HOMO = \Delta LUMO \neq 0$ obtains almost identically for the pyridinate complex of zinc octaethylchlorin. The mixed MCD sign pattern observed for the Q_0^y transition may be viewed as arising from the incipient "takeover" of the μ^+ pattern $(+[\theta]_M)$ from that of the μ^- $(-[\theta]_M)$ pattern. In the Q_0^x transition, on the other hand, the contributions from the μ^- *and* μ^+ moments reinforce each other and give rise to the relatively strong negative MCD band. The pattern in the Soret is clearly that of the μ^- contribution (i.e., $-+$).

The condition of almost soft for the chlorin chromophore can also be modulated in a very subtle way by varying the number of peripheral alkyl substituents. As an example, notice in the structural formula of zinc bonellin (Figure 8) that rings I and II each have only one alkyl substituent, whereas two are present for each in zinc octaethylchlorin. It would stretch the credibility of our protocol to attempt to quantitatively account for the effects of two fewer weak $-E$ alkyl perturbers; however, for heuristic purposes we do note that four alkyl groups contribute to the rise in the energy of the b_2 orbital of bonellin as compared to six for octaethylchlorin. In the LUMO's (Figure 2) three and one (instead of four and two) alkyl perturbers are effective in raising the levels of the c_2 and c_1 orbitals, respectively. Qualitatively, for bonellin dication these shifts might be expected to make the quantity $\Delta HOMO - \Delta LUMO$ only slightly more negative than was the case for octaethylchlorin dication. Consequently, the fact that bonellin dication and octaethylchlorin dication exhibit nearly identical MCD spectra is not surprising. The effects of variation in the number of alkyl groups are a little more subtle and difficult to judge for the zinc complexes. However, on the basis of the observed MCD band sign pattern of zinc bonellin (Figure 8) and the attribution of either the μ^+ pattern $(-+-+)$ for the visible and Soret MCD bands or else, equivalently, the μ^+ pattern for the visible and the μ^- pattern for the Soret, we conclude that $\Delta HOMO > \Delta LUMO$ for zinc bonellin just as was concluded above for zinc octaethylchlorin. Evidently, however, $\Delta HOMO$ is smaller for zinc bonellin than for zinc octaethylchlorin since upon ligation with pyridine the sign of the Q_0^y MCD band of zinc bonellin changes from negative to positive (Figure 8), whereas in the case of zinc octaethylchlorin the sign of this band was mixed (Figure 7). Thus, for the pyridinate complex of zinc bonellin, in distinction to that of zinc octaethylchlorin, the positive μ^+ sign for the Q_0^y band clearly overwhelms the weaker negative sign of the μ^- contribution. The Q_0^x MCD band has the expected negative sign. In the Soret region the observed $-+$ MCD band sign pattern must again be attributed to the μ^- contribution.

The effect of pyrrole alkyl substituents in raising the energy of the chlorin b_2 orbital can also be seen in the free-base series (Figure 5). Here the net effect of the alkyl perturbers is to increase the spacing between the HOMO's relative to that between the LUMO's. Thus, the Q bands of chlorin show the inverted pattern (Figure 3, Part 1[1]), whereas those of octaethylchlorin (Figure 4, Part 1) and bonellin (Table I, Part 1) have the normal sign pattern.

(iii) Bacteriochlorins. A central thread in our discussion of structure–spectra correlations in the preceding sections has been the occurrence of energy level distribution situations for which the quantity $|\Delta HOMO - \Delta LUMO|$ is small. These conditions lead to the possibility of substituent-induced sign variation in the MCD spectra of a closely related series of compounds and examples of double soft, soft, and almost soft MCD chromophores have been cited and discussed. In the bacteriochlorin series we encounter examples of the hard MCD chromophore case wherein substituent-induced sign variations are not likely to occur.

In the bacteriochlorin macrocycle (see structures given in Figures 6 and 7 of Part 1[1]) the ethylenic double bonds in rings II and IV are both removed by reduction from the normal π system of porphyrins. From the representation of the four-orbital MO's of porphin given in Figure 2 it can be seen that these two chlorin perturbations should affect the energies of the c_1 and b_2 orbitals much more strongly than those of the c_2 and b_1 orbitals since for the latter two there is little electron density at the sites of reduction. We assume, consistent with results of MO calculations,[11c] that the increases in orbital energies owing to the chlorin perturbations are additive; consequently, in bacteriochlorins the LUMO's should be inherently much more widely split than the HOMO's. Because of this, we predict (Figures 3–5) that bacteriochlorins should show the inverted $+-+-$ pattern for the MCD bands associated with their four lowest-energy electronic transitions regardless of the peripheral or central substituent present. This prediction is confirmed with certainty for the Q bands of all of the bacteriochlorins investigated (Table I). The prediction does not, however, fit well the experimental spectra in the Soret region since a positive shoulder or peak may appear between the predicted positive and negative Soret MCD bands in both the octaethyl- and tetraphenylbacteriochlorin series (Figures 6 and 7, Part 1[1]).

There is, however, notwithstanding the prediction of an invariant sign pattern for bacteriochlorins, structural information that can be garnered from their MCD spectra. As a specific example, compare the orbital energy level diagrams adduced for tetraphenylbacteriochlorin and octaethylbacteriochlorin free base in Figure 5. We forego a description of how the diagrams were constructed and note only that $|\Delta HOMO - \Delta LUMO|$ is much larger in the case of tetraphenylbacteriochlorin than it is for the octaethyl derivative. This difference should be, and is, reflected in their MCD spectra since, for example, $B(Q_0^y) = -10.34\ D^2\ \beta_e/10^3\ cm^{-1}$ for the former and $-2.53\ D^2\ \beta_e/10^3\ cm^{-1}$ for the latter.[39]

(iv) Isobacteriochlorins. In the preceding sections on porphyrins, chlorins, and bacteriochlorins we found that our protocol for the application of Michl's perimeter model achieved a uniform degree of success. No major failures, i.e., incorrect predictions for the Q bands, were encountered, and in fact, the protocol was able to account successfully for the MCD band sign inversions that attend some rather subtle substituent effects in the chlorin series. In the isobacteriochlorin series we encounter for the first time a major problem with the *direct application* of our protocol in that, as signalled by the double asterisk in Figures 3–5, we are not able to correctly predict the MCD band sign pattern of the tetraphenylisobacteriochlorins.

Before considering the source of this problem and how it can be dealt with, it is useful to first examine the way in which our protocol has led to the orbital energy level diagrams shown for the isobacteriochlorins in Figures 3–5. The isobacteriochlorin ring system (see structures given in Figures 8 and 10 of Part 1[1]) is distinguished from that of the bacteriochlorin macrocycle by the fact that the ethylenic double bonds in adjacent rather than in opposed rings are reduced. Thus, for the orbital energy level diagram shown in Figure 4 for isobacteriochlorin dication to be arrived at, two adjacent chlorin perturbations are applied to the MO's of porphine dication. The removal of the ethylenic unit in ring IV from the π system raises the energy of the e_g1 orbital, whereas removal of the one in ring I raises the energy of the e_g2 orbital. Both chlorin perturbations are counted as raising the energy of the a_{1u} orbital. As noted in the protocol section, we have sought a straightforward experimental basis for our procedures and so proposed to count each of the two chlorin perturbations as having an equal affect on the energy levels. The result of this procedure is, as shown in Figure 4, that while the HOMO's of unsubstituted isobacteriochlorin dication are split, the LUMO's are predicted to be accidentally degenerate. On this basis, we make the prediction in Figure 4 that the normal, $-+-+$, MCD band sign pattern should be observed for the four lowest energy purely electronic transitions of isobacteriochlorin dication. This is, in fact, the pattern observed for octaethylisobacteriochlorin dication (Table I).

Thus, our protocol does lead to a prediction that would be consistent with the MCD band sign pattern that is actually observed in the alkyl isobacteriochlorins. However, in the tetraphenyl series the straightforward application of our procedures leads to an unhappy result. In particular, notice that, starting from the energy-level diagram for porphine dication shown in Figure 4, the initial application of the *meso*-tetraphenyl perturbation leads to an increase in the energy of the a_{2u} orbital but leaves the relative energy disposition of the LUMO's unaltered. Next, application of the two chlorin perturbations in the manner prescribed raises the energy level of the a_{1u} orbital by the same amount. Consequently, the descendants of these orbitals in tetraphenylisobacteriochlorin dication, the b_1 and b_2 orbitals, respectively, are predicted to be accidentally degenerate. Furthermore as stated before, the application of the two chlorin perturbations in adjacent rings leaves the LUMO orbitals accidentally degenerate as well. The result is that, as shown in Figure 4, $\Delta\text{HOMO} \simeq \Delta\text{LUMO} \simeq 0$, and if exactly so, we would be forced to predict (square brackets in Table I) that for tetraphenylisobacteriochlorin dication or dianion the μ^- moment contributions alone would determine the MCD band sign pattern in the Soret and that the MCD would vanish in the visible bands. This prediction is not consonant with experiment since our MCD spectra (Table I) show that the MCD bands of tetraphenylisobacteriochlorin dication are inverted in both the Soret and visible regions. Furthermore, as shown in Figure 10 of Part 1,[1] the visible bands of the free-base and zinc derivatives of tetraphenylisobacteriochlorin are also inverted, whereas our protocol predicts that they should be normal in sign pattern. These MCD band sign inversions found experimentally mean that, assuming the validity of Michl's treatment, the LUMO's of the isobacteriochlorin chromophore must, in fact, be split.

This conclusion that, in contradistinction to the results of a low order perturbation treatment, the LUMO's of the isobacteriochlorin chromophore are split also comes out of the several explicit MO calculations which have been reported[11,25,40] for this macrocycle.

The numerical calculations for the unsubstituted isobacteriochlorin macrocycle, however, produce the condition that $\Delta\text{HOMO} > \Delta\text{LUMO}$ which is, as noted, consistent only with our experimental MCD data for the alkyl isobacteriochlorin series. Consequently, it is important to determine if the calculated splitting in the LUMO's can be introduced on an ad hoc basis into our perturbation treatment in a way that will also permit a rationalization of the sign inversions in the tetraphenyl series. In Figure 9b the distributions of the HOMO's and LUMO's for "metal" isobacteriochlorin obtained from the SCMO-PPP calculation of Weiss, Kobayashi, and Gouterman[11c] are reproduced. Other calculations such as the IEH calculation of Hanson and coworkers[40] indicate an even wider split in the LUMO's with the consequence that ΔHOMO and ΔLUMO are more nearly equal in magnitude than is shown in Figure 9.

An, at least intuitively, appealing perturbation procedure is to first introduce the effects of the phenyl, alkyl, central substituent, and chlorin perturbations on the HOMO's of the reference porphyrin and then to introduce the calculated splitting of the LUMO's by the two chlorin perturbations. This procedure has been followed in generating the orbital energy level diagrams shown for the isobacteriochlorin dianions in Figure 9. In octaethylisobacteriochlorin dianion (Figure 9c) the condition of $\Delta\text{HOMO} > \Delta\text{LUMO}$, required by experiment, is maintained and significant variations in the MCD spectra owing to the effects of central substituents would not be expected. In fact, the MCD spectra of the alkyl isobacteriochlorins (free-base, dication, and zinc complexes) are all remarkably similar. However, a specific calculation will be required to account for the observation that the MCD of the lowest-energy Q band is oppositely signed for the two proton tautomers of the free-base alkyl-substituted isobacteriochlorins as is indicated by the low-temperature spectrum shown in Figure 9 of Part 1.[1] The diagram for tetraphenylisobacteriochlorin dianion (Figure 9a) suggests that fairly subtle central substituent effects are more likely to be evident than in the alkyl series. Thus, substitution of four protons at the core of tetraphenylisobacteriochlorin dianion should not lower the energy of the b_1 orbital significantly, and we predict that the contribution of the μ^+ moment should dominate and lead to the $+-+-$ (prediction in braces in Table I) MCD band pattern. This is, indeed, the pattern that is observed experimentally. In the zinc complex the HOMO's should be more widely split than is shown in Figure 9a owing to the lowering in energy of the b_1 orbital due to the electron-withdrawing effect of zinc. Now the condition of $\Delta\text{HOMO} \approx \Delta\text{LUMO}$ obtains, and it is not surprising that in Table I it is necessary to modify the μ^+ prediction shown in braces with that of the μ^- prediction for the Soret bands. This viewpoint is supported by our experimental observation that ligation of the zinc complex of tetraphenylisobacteriochlorin with pyridine gives rise (because of the consequent increase in the energy of the b_1 orbital) to an MCD spectrum in which the MCD bands in *both* the Soret and visible regions are inverted. In tetraphenylisobacteriochlorin free base the two central protons also modulate the splitting in the HOMO's with the result that it is again necessary to consider μ^- contributions for the Soret MCD bands.

(v) Applications to Other Substituted Reduced Porphyrins. Michl's perimeter model and the notions developed and illustrated in the preceding sections of this paper can also be fruitfully employed for first-order structure elucidations in other reduced porphyrin derivatives.

In a preliminary communication[41] we pointed out that two low-spin derivatives of the iron(II) chlorin heme d_1 (**1**) exhibit[42,43]

(40) Chang, C. K.; Hanson, L. K.; Richardson, P. F.; Young, R.; Fajer, J. *Proc. Natl. Acad. Sci. U.S.A.* **1981**, *78*, 2652–2656.

(41) Keegan, J. D.; Stolzenberg, A. M.; Lu, Y. C.; Linder, R. E.; Barth, G.; Bunnenberg, E.; Djerassi, C.; Moscowitz, A. *J. Am. Chem. Soc.* **1981**, *103*, 3201–3203.

(42) Vickery, L. E.; Palmer, G.; Wharton, D. C. *Biochem. Biophys. Res. Commun.* **1978**, *80*, 458–463.

the normal MCD band sign pattern in the visible region and that this event, in the light of the usually inverted pattern observed for all of the examples in the literature *up until that time*, was unexpected. If we assume that low-spin ferrous iron is not less electron withdrawing than zinc, then the orbital energy level diagram of zinc octaethylchlorin shown in Figure 3 can serve as a reference point. Project the structure of ferrous heme d_1 (**1**) onto the diagrams of the molecular orbitals of porphin shown in Figure 2 and note that the essential difference between heme d_1 and zinc octaethylchlorin is that a vinyl group replaces an ethyl group in ring II. The vinyl group is not a strongly perturbing porphyrin substituent. Evidently, the combined effect of low-spin iron(II), the alkyl groups, and the vinyl group is such that the condition $\Delta HOMO > \Delta LUMO$ proposed in Figure 3 for zinc octaethylchlorin is maintained.

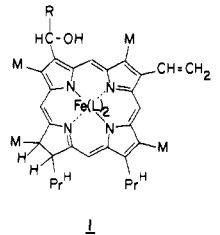

1

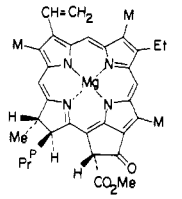

2 (P = PHYTYL)

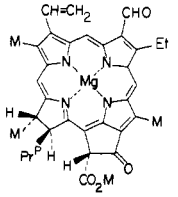

3 (P = PHYTYL)

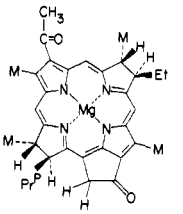

4 (P = PHYTYL)

As a second example, we consider the MCD spectra expected for chlorophyll *a* (**2**) and chlorophyll *b* (**3**). Since magnesium does not have low-lying π orbitals, we use the orbital energy level diagram shown for octaethylchlorin dication in Figure 4 as a common reference compound. We neglect the effect of the meso alkyl and vinyl substituents and further assume that, for our present heuristic purposes, the effects of the strong $+E$ carbonyl substituent(s) do not exceed the bounds of our perturbation treatment. In the case of chlorophyll *a* (**2**) the carbonyl substituent is located on ring III. Thus, with reference to the MO's represented in Figure 2, the energy levels of the c_2 and b_2 orbitals should both be lowered with the larger change being that of the LUMO. Since $\Delta LUMO$ is increased and $\Delta HOMO$ decreased, we predict that the condition of $\Delta HOMO < \Delta LUMO$ already present for the octaalkyl dication will be reinforced, that chlorophyll *a* should exhibit the inverted pattern, and that its MCD bands will be more intense than the corresponding ones of octaethylchlorin dication. The predicted inverted pattern is, in fact, observed experimentally.[44] In addition, $[\theta]_M(Q_0^y) \simeq +15$ deg cm^2 dmol^{-1} G^{-1} for chlorophyll *a*,[44] whereas the corresponding value for octaethylchlorin dication is +2.9.[1] A somewhat different distribution of energy levels is projected for chlorophyll *b* (**3**) owing to the replacement of a methyl group in ring II by the $+E$ formyl group. With reference to Figure 2, it can be seen that the perturbation owing to the formyl group, in addition to the perturbations already counted for chlorophyll *a* above, should be to lower the energies of the c_1 and b_2 orbitals. The split in the LUMO's is decreased and the quantity $|\Delta HOMO - \Delta LUMO|$ should be smaller for chlorophyll *b* than for chlorophyll *a*. Consequently, it is not surprising that the MCD of chlorophyll *b* is inverted or that the ratio $[\theta]_M(Q_0^y$, Chl *a*$)/[\theta]_M(Q_0^y$, Chl *b*$)$ is about 2.[44] A similar line of reasoning can be used to explain the inverted MCD bands we reported in our early study[45] of the electronic spectra of free-base chlorins bearing electron-withdrawing substituents.

On the basis of arguments just made for heme d_1, the chlorophylls, and those made in section ii for the chlorins studied in this work, we conclude that, while the chlorin perturbation can, of itself, give rise to sign inversion, the more general causative structural features are the presence of either electron-withdrawings groups in rings I and/or III or else electron-donating groups (e.g., four phenyls) at the meso positions. Electronegative substituents in ring II only should give rise to the normal sign pattern.

As the final example, assuming again that the carbonyl groups in the bacteriochlorophyll *a* molecule (**4**) leave the transition moments of the Q_0^y and Q_0^x transitions nominally along the *y* and *x* axes as is indicated by Petke, et al.[22] and that the central magnesium and dication substituents are comparable, we note from Figure 2 that the effect of placing the $+E$ carbonyl substituents in rings I and III should be to lower the energies of the c_2 and b_2 orbitals. Thus, in comparison to the energy-level diagram of octaethylbacteriochlorin dication shown in Figure 4, the one projected for bacteriochlorophyll *a* should show an even wider split in the LUMO's and a narrower one in the HOMO's. This prediction that $|\Delta HOMO - \Delta LUMO|$ is larger for the naturally occurring derivative than for the synthetic one is compatible with Sutherland and Olson's[46] value of $B(Q_0^y) = -12.5$ D^2 $\beta_e/10^3$ cm^{-1} for bacteriochlorophyll *a* (in methanol) as compared to our[39] value of -3.6 D^2 $\beta_e/10^3$ cm^{-1}.

Recently, Stolzenberg et al.[47] have published the MCD spectra of some high-spin, five-coordinate complexes of iron(III) octaethylisobacteriochlorin. Although the MCD spectra of these complexes could be complicated by the presence of nonzero *C* terms, which are not included in Michl's theoretical development of the perimeter model, the spectra presented[47] are similar in appearance to that of the diamagnetic zinc complex given in Figure 8 of Part 1.

Summary. In the present work, we have investigated a series of unsubstituted, octaalkyl-substituted, and tetraphenyl-substituted chlorins, bacteriochlorins, and isobacteriochlorins in an effort to critically test Michl's perimeter model[7] for relating the absolute signs of the lowest energy purely electronic MCD bands of cyclic π-electron systems to their molecular structures.

Because of the potential utility of the model for use among porphyrin chemists, we have adopted a very simple protocol that avoids the need for numerical calculations. This procedure effectively syncretizes the elements of an experimental basis and the classic concepts of Gouterman's[11] four-orbital model of porphyrin states.

We find Michl's model and, concomitantly, our protocol for its application to be very useful for understanding the causes of the substituent-induced sign variations that occur in the chlorin and isobacteriochlorin series and for understanding why the sign pattern of bacteriochlorins can be expected to be invariant regardless of its substituents. The absolute signs of the Q_0^y and Q_0^x MCD bands are correctly predicted by direct application of our protocol for all series with the exception of the tetraphenylisobacteriochlorins for which resort to the results of an MO calculation is required in order to adequately fit the data. It is more difficult to unambiguously test Michl's assertions in the Soret region because of the interplay between μ^- and μ^+ contributions. Our results for this region are, however, generally consistent with the tenets of the model with a few exceptions where it is clear that the four-orbital precept of the composition of this band breaks down.

In conclusion, we believe that Michl's perimeter model should find widespread use among porphyrin chemists as a first-order

(43) Walsh, T. A.; Johnson, M. K.; Greenwood, C.; Barber, D.; Springall, J. P.; Thomson, A. J. *Biochem. J.* **1979**, *177*, 29–39.
(44) Schreiner, A. F.; Gunter, J. D.; Hamm, D. J.; Jones, I. D.; White, R. C. *Inorg. Chim. Acta* **1978**, *26*, 151–155.
(45) Briat, B.; Schooley, D. A.; Records, R.; Bunnenberg, E.; Djerassi, C. *J. Am. Chem. Soc.* **1967**, *89*, 6170–6177.
(46) Sutherland, J. C.; Olson, J. M. *Photochem. Photobiol.* **1981**, *33*, 379–384.
(47) Stolzenberg, A. M.; Strauss, S. H.; Ham, R. H. *J. Am. Chem. Soc.* **1981**, *103*, 4763–4778.

approach for structure–spectra correlations and as a conceptual tool for designing further spectroscopic studies.

Acknowledgment. We with to thank Professor R. H. Holm for his interest in this project and Ruth Records for her assistance with the measurements. Y.-C.L. was a visiting scholar from the Beijing Institute of Chemical Reagents. A.M.S. was a predoctoral fellow of the Fannie and John Hertz Foundation. Financial support for this research was provided by grants from the National Science Foundation (CHE-77-04397 and CHE-80-09240) and the National Institutes of Health (GM-20276 and HL-16833).

Registry No. P^{2-}, 30882-36-1; PH_2, 101-60-0; PH_4^{2+}, 20910-09-2; ZnP, 14052-02-9; TPP^{2-}, 32796-32-0; $TPPH_2$, 917-23-7; $TPPH_4^{2+}$, 50849-35-9; ZnTPP, 14074-80-7; OEP^{2-}, 52985-81-6; $OEPH_2$, 2683-82-1; $OEPH_4^{2+}$, 24804-25-9; ZnOEP, 17632-18-7; CH_2, 2683-84-3; CH_4^{2+}, 82135-15-7; ZnC, 77124-66-4; ZnC·pyr, 82135-40-8; $OECH_2$, 991-74-2; $OECH_4^{2+}$, 82135-16-8; ZnOEC, 28375-45-3; ZnOEC·Pyr, 82149-91-5; $TPCH_2$, 2669-65-0; $TPCH_4^{2+}$, 50849-36-0; ZnTPC, 14839-32-8; BCH_2, 2683-78-5; BCH_4^{2+}, 82135-17-9; ZnBC, 78802-04-7; $TPBCH_2$, 5143-18-0; $TPBCH_4^{2+}$, 82113-35-7; ZnTBC, 50795-70-5; $OEPBCH_2$, 23016-64-0; $OEBCH_4^{2+}$, 82113-34-6; ZnOEBC, 82135-39-5; iBC^{2-}, 82113-48-2; $iBCH_2$, 67883-10-7; $iBCH_4^{2+}$, 82113-49-3; ZniBC, 79008-66-5; $TPiBC^{2-}$, 82113-50-6; $TPiBCH_2$, 25440-13-5; $TPiBCH_4^{2+}$, 82113-37-9; ZnTPiBC, 14705-64-7; $OEiBC^{2-}$, 82113-51-7; $OEiBCH_2$, 72260-12-9; $OEiBCH_4^{2+}$, 82113-36-8; ZnOEiBC, 39001-89-3; zinc bonellin, 82135-38-4; zinc bonellin·pyr, 82149-92-6.

Thermochemistry of Group 4A Isobutene Analogues by Pulsed Ion Cyclotron Double Resonance Spectroscopy

William J. Pietro and Warren J. Hehre*

Contribution from the Department of Chemistry, University of California, Irvine, California 92717. *Received December 21, 1981*

Abstract: Pulsed ion cyclotron double resonance spectroscopy has been employed to obtain heats of formation of 1,1-dimethylsilaethylene (7 kcal mol^{-1}), 1,1-dimethylgermaethylene (6 kcal mol^{-1}), 1,1-dimethylstannaethylene (31 kcal mol^{-1}), and 1,1-dimethylplumbaethylene (59 kcal mol^{-1}), neutral products derived from proton abstraction from the corresponding trimethylsilyl, trimethylgermyl, trimethylstannyl, and trimethylplumbyl cations in the gas phase. These data, combined with estimates for the heats of formation of the corresponding biradical forms (obtained from the heats of formation of the tetramethyl compounds, $M(CH_3)_4$, and estimates of CH and MC bond dissociation energies), yield π-bond energies of 38, 43, 45, and 30 kcal mol^{-1} for the four olefin analogues, respectively.

The apparent absence of multiple bonding in the higher group 4A elements is a well-known and intriguing phenomenon. Compounds incorporating multiple bonds between carbon and other first-row elements are commonplace, while stable, isolable congeners involving silicon are rare[1] and (as yet) nonexistent for germanium, tin, and lead. Olefin analogues of higher group 4A elements have, however, been proposed as transient species or short-lived intermediates in many reactions.[2] For example, the observation that pyrolysis of 1,1-dimethylsilacyclobutane results in the formation of the corresponding tetramethyl-1,3-disilacyclobutane may best be rationalized in terms of the intermediacy of 1,1-dimethylsilaethylene (**1**).[3] Further support for such a

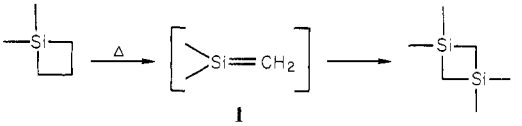

1

mechanism may be found in the work of Grinberg,[4] who reported that pyrolysis of a mixture of 1,1-dimethylsilacyclobutane and the bis(deuteriomethyl-d_3) derivative led to all three possible dimerization products. The silaethylene intermediate has also been chemically trapped by carrying out the pyrolysis in the presence of ammonia, water, and alcohols.[5] Other agents (e.g., phenols, amines, and nitriles) have also been employed as chemical traps.[6] The proposed silaethylene intermediate has also been made to undergo [2 + 2] and [2 + 4] cycloaddition upon pyrolysis in the presence of olefins and dienes.[7] [2 + 2] cycloaddition products have also been detected when ketones, thioketones, and imines were used in place of olefins.[6a,8] By rapidly immobilizing the very-low pressure pyrolysis products of 1,1,3-trimethyl-1-silacyclobutane on a frozen argon matrix, Maltsev and co-workers,[9] among others, have obtained infrared spectra of **1**. Koenig and McKenna[10] have recorded the photoelectron spectrum of 1,1-dimethylsilaethylene, and Montgomery and co-workers[11] have determined its structure by electron diffraction.

Numerous reports have appeared that strongly implicate the existence of other short-lived intermediates containing formally unsaturated silicon.[2] Among the most interesting are molecules related to silabenzene.[12]

Pyrolysis of 1,1-dimethylgermacyclobutane does not, as might be expected, result in cyclodimerization products of intermediate

(1) A. G. Brook, presented at the 15th Annual Organosilicon Symposium, Durham, NC, 1981.
(2) For a recent review, see: L. E. Gusel'nikov and N. S. Nametkin, *Chem. Rev.*, **79**, 531 (1979).
(3) N. S. Nametkin, V. M. Vdovin, L. E. Gusel'nikov, and V. I. Zav'yalov, *Izv. Akad. Nauk SSSR, Ser. Khim.*, 584 (1966).
(4) P. L. Grinberg, Ph.D. Thesis, Topchiev Institute of Petrochemical Synthesis, Academy of Science, Moscow, 1969.
(5) (a) M. C. Flowers and L. E. Gusel'nikov, *J. Chem. Soc. B*, **419**, 1296 (1968). (b) L. E. Gusel'nikov, *J. Chem. Soc.*, **5**, 23 (1968). (c) N. S. Nametkin, L. E. Gusel'nikov, W. M. Vdovin, P. L. Grinberg, V. I. Zav'yalov, and V. D. Oppengeim, *Dokl. Akad. Nauk SSSR*, **171**, 630 (1966).
(6) (a) R. D. Bush, C. M. Golino, G. D. Homer, and L. H. Sommer, *J. Organomet. Chem.*, **80**, 37 (1974). (b) R. D. Bush, C. M. Golino, D. N. Roark, and L. H. Sommer, *J. Organomet. Chem.*, **59**, C17 (1973).
(7) (a) N. S. Nametkin, L. E. Gusel'nikov, R. L. Ushakova, and V. M. Vdovin, *Izv. Akad. Nauk SSSR, Ser. Khim.*, 1840 (1971). (b) N. S. Nametkin, L. E. Gusel'nikov, R. L. Ushakova, and V. M. Vdovin, *Dokl. Akad. Nauk SSSR*, **201**, 1365 (1971).
(8) (a) D. N. Roark and L. H. Sommer, *J. Chem. Soc., Chem. Commun.*, 167 (1973). (b) C. M. Golino, R. D. Bush, D. N. Roark, and L. H. Sommer, *J. Organomet. Chem.*, **66**, 29 (1974). (c) L. H. Sommer and J. McLick, *J. Organomet. Chem.*, **101**, 171 (1975). (d) C. M. Golino, R. D. Bush, and L. H. Sommer, *J. Am. Chem. Soc.*, **96**, 614 (1974).
(9) A. K. Maltsev, V. N. Khabashesku, and O. M. Nefedov, *Izv. Akad. Nauk SSSR, Ser. Khim.*, 1193 (1976).
(10) T. Koenig and W. McKenna, *J. Am. Chem. Soc.*, **103**, 1212 (1981).
(11) P. G. Mahaffy, R. Gutowsky, and L. K. Montgomery, *J. Am. Chem. Soc.*, **102**, 2854 (1980).
(12) T. J. Barton and D. S. Banasiak, *J. Am. Chem. Soc.*, **99**, 5199 (1977).

0002-7863/82/1504-4329$01.25/0